Plant & Cell Physiology 60 (5): 1025-1040 (2019)

# Tissue Distribution and Specific Contribution of *Arabidopsis* FAD7 and FAD8 Plastid Desaturases to the JA and ABA Mediated Cold Stress or Defence Responses

**Running head:** non-redundant FAD7 and FAD8 responses to stress

**Corresponding author**: M. Alfonso; Department of Plant Nutrition, Estación Experimental de Ala Dei-Consejo Superior de Investigaciones Científicas (CSIC), Avda Montañana 1005, 50059 Zaragoza, SPAIN. Tel: +34 976 71 60 59; Fax: +34 976 716045; E-mail address: alfonso@eead.csic.es

**Subject area:** (4) proteins, enzymes and metabolism; (2) environmental and stress responses.

**Number of figures**: 8; black and white: 4; colour figures: 4.

**Number of tables:** 1.

**Supplementary material:** 8 figures, 1 table.

# Tissue Distribution and Specific Contribution of *Arabidopsis* FAD7 and FAD8 Plastid Desaturases to the JA and ABA Mediated Cold Stress or Defence Responses

**Running head:** non-redundant FAD7 and FAD8 responses to stress

Ángel Soria-García[1], María C. Rubio[1], Beatriz Lagunas[2], Sara López-Gomollón[3], María de los Ángeles Luján[1], Raúl Díaz-Guerra[1], Rafael Picorel[1] and Miguel Alfonso[1,*]

[1]Department of Plant Nutrition, Estación Experimental Aula Dei (EEAD-CSIC).

Avda. Montañana 1005, 50059 Zaragoza, Spain.

[2]School of Life Sciences, University of Warwick, Gibbet Hill Road, Coventry, CV4 7AL, UK.

[3]Department of Plant Sciences, University of Cambridge, Downing Street, Cambridge, CB2 3EA, UK.

*Corresponding author: M. Alfonso, Department of Plant Nutrition, Estación Experimental de Ala Dei-Consejo Superior de Investigaciones Científicas (CSIC), Avda Montañana 1005, 50059 Zaragoza, SPAIN. Tel: +34 976 71 60 59; Fax: +34 976 716045; E-mail address: alfonso@eead.csic.es

**Abbreviations**: ABA, absicic acid; ACP, acyl-carrier protein: BiFC, bimolecular fluorescence complementation; DA. dienoic fatty acids; DGDG, digalactosyl-diacylglycerol; ER, endoplasmic reticulum; FAE, fatty acid elongase; FAS, fatty acid synthase; GFP, green fluorescent protein; GUS, glucuronidase; JA, jasmonate; LOX, lipooxigenase; MGDG, monogalactosil-diacylglycerol; PG, phosphatidyl-glicerol; RT-qPCR, quantitative real-time PCR; TA, trienoic fatty acid; YFP, yellow fluorescent protein.

To overcome the difficulties to analyze membrane desaturases at the protein level, transgenic Arabidopsis plants expressing the plastidial *At*FAD7 and *At*FAD8 ω-3 desaturases fused to GFP, under the control of their endogenous promoters, were generated and their tissue relative abundance was studied. Gene expression, GUS promoter activity, immunoblot and confocal microscopy analyses indicated that *At*FAD7 is the major ω-3 desaturase in leaves when compared to *At*FAD8. This higher abundance of *At*FAD7 was consistent with its higher promoter activity and could be related with its specificity for the abundant leaf galactolipids. *At*FAD7 was also present in roots but at much lower level than leaves. *At*FAD8 expression and protein abundance in leaves was consistent with its lower promoter activity, suggesting that transcriptional control modulates the abundance of both desaturases in leaves. *At*FAD7 protein levels increased in response to wounding but not to JA, and decreased upon ABA treatment. Conversely, *At*FAD8 protein levels increased upon cold or JA exposure and decreased at high temperatures, but did not respond to ABA or wounding. These results indicated specific and non-redundant roles for the plastidial ω-3 desaturases in defence, temperature stress or phytohormone mediated responses and a tight coordination of their activities between biotic and abiotic stress signalling pathways. Our data suggested that transcriptional regulation was crucial for this coordination. Finally, bimolecular fluorescence complementation analysis showed that both *At*FAD7 and *At*FAD8 interact with the *At*FAD6 ω-6 desaturase *in vivo*, suggesting that quaternary complexes are involved in trienoic fatty acid production within the plastid membranes.

**Keywords:** *Arabidopsis thaliana*, fatty acid, FAD7, FAD8, ABA, cold, JA, wounding.

## Introduction

Trienoic fatty acids (TAs) are key components of the plant responses against biotic and abiotic stress. As major constituents of plant glycerolipids (Browse et al., 1986), they influence the function of biological membranes by maintaining their appropriate fluidity, playing a key role in plant adaptation to temperature changes (Iba, 2002). The relationship between the unsaturation of membrane lipids and temperature acclimation has been stablished in the past (Nishida and Murata, 1996; Iba, 2002). In addition, certain lipids like phosphatidilglycerol (PG) have been directly linked to chilling sensitivity (Murata et al., 1982). TAs also serve as precursors of plant hormones, like jasmonates, that are directly involved in defence signalling against pathogen attack, participate in the wound response and are also important for plant development and adaptation to environmental stress (Schaller and Stinzi, 2009). Biosynthesis of jasmonates is initiated in the plastid through the action of specific lipases that release TAs from the glycerol backbone making them accessible to lipooxigenases (LOX), that initiate the conversion of these TAs to jasmonates (Wasternack and Hause, 2013).

TAs are synthesized from dienoic fatty acids (DAs) by the activity of ω-3 desaturases that are a family of integral membrane enzymes localized in two different cell compartments: FAD3 is specific of the endoplasmic reticulum (ER; Dyer and Mullen, 2001) while FAD7 and FAD8 are plastid specific (Browse et al., 1986; Román et al., 2015). In Arabidopsis, ω-3 fatty acid desaturases are encoded by single genes (Yadav et al., 1993; Gibson et al., 1994) while in other plant species like soybean, several isoforms of the microsomal and plastidial ω-3 fatty acid desaturases have been reported (Bilyeu et al., 2003; Andreu et al., 2010; Román et al., 2015). Both plastidial ω-3 desaturases, FAD7 and FAD8, are highly homologous (more than 90% identity at the protein sequence level), and perform a similar function in the same sub-cellular compartment, the plastid envelope (Román et al., 2015). It was initially reported that FAD8 was a cold-specific desaturase (McConn et al., 1994). However, recent analysis of a collection

of loss-of-function mutants from Arabidopsis for the *AtFAD7* and *AtFAD8* genes revealed that *At*FAD8 is also active at control growth temperatures and differences in substrate specificity at polar lipid head group (FAD8 showed preference for PG and sulfolipids) and acyl chain length (FAD7 uses both 16:2 and 18:2 as substrates while FAD8 uses only 18:2 substrates) existed (Román et al., 2015). These data also indicated that *At*FAD8 was active at normal temperatures and could compensate, at least partially, the absence of a functional *At*FAD7 enzyme at 22 ºC (Román et al., 2015), implying the presence of a functional *At*FAD8 protein at 22 ºC. This non-redundant role of both plastidial ω-3 desaturases in the biosynthesis of TAs in the plastid (Roman et al., 2015), could be extended to their participation in plant responses to biotic or abiotic stress. Thus, the wound responsive pattern of the *FAD7* gene has been reported in different plant species, consistent with the increasing demand of TAs for JA biosynthesis (Hamada et al., 1996; Nishiuchi et al., 1997; Reymond et al., 2000). However, no data are available of the responsiveness of the *FAD8* gene to JAs or in defense responses. On the other hand, induction of *FAD8* gene expression at low temperatures has also been reported (McConn et al., 1994; Berberich et al., 1998; Román et al., 2015), consistent with a higher ω-3 desaturase activity on plastid lipids to maintain plastid membrane fluidity. The use of *myc*-tagged FAD7 and FAD8 proteins expressed in Arabidopsis indicated that protein stability might contribute to the FAD8 role at low temperatures (Matsuda et al., 2005). However, there has been no experimental support showing that translation is the key regulatory mechanism controlling the activity of the FAD8 enzyme in response to cold. Nevertheless, we are still far from understanding how the activity of both plastidial ω-3 desaturases is specifically regulated in response to these stimuli. Most of our conclusions were obtained through the correlation of *FAD* gene expression levels with changes in the fatty acid content (Gibson et al., 1994; Berberich et al., 1998; Collados et al., 2006; Martz et al., 2006; Román et al., 2012; Lagunas et al., 2013; Roman et al., 2015). However, our comprehension of desaturase function at the

protein level and more concretely, the relative abundance of FAD7 and FAD8 proteins in the different plant tissues and organs, as well as their variation in response to environmental or developmental stimuli are poorly understood. This analysis of desaturase regulation at the protein level is hampered by their high degree of homology as well as their high hydrophobicity, limiting the utilization of specific antibodies or the development of purification protocols. In addition, transgenic lines that expressed the protein under constitutive promoters like 35S (Matsuda et al., 2005; Román et al., 2015), were useful for localization purposes but their protein levels did not represent their actual regulation. This limits our comprehension of the relevance of translation or post-translational mechanisms in the regulation and coordination of plastidial ω-3 desaturases to stress or hormone responses. Question arises whether the different responses of both plastidial ω-3 desaturases is regulated mainly at the transcriptional level, through the action of specific transcription factors, or are post-transcriptional regulatory mechanisms behind some of these specific responses. Furthermore, much of the data are focused in leaves, but very little information, if any, is available about the relative abundance and function of both plastid ω-3 desaturases in other plant tissues and organs like roots or flowers where TAs, as precursors of JA, participate in developmental processes like root elongation or pollen development (Staswick et al., 1992; McConn and Browse, 1996).

In this work, we tried to overcome some of the above-mentioned issues using stable transgenic lines of *Arabidopsis thaliana* that express both *At*FAD7 and *At*FAD8 proteins fused to a green fluorescent protein (GFP) under the control of their endogenous promoter sequences. This strategy allowed us to distinguish both *At*FAD7 and *At*FAD8 proteins, which are highly identical at the protein sequence level, and analyze their regulation. Data obtained with these lines, together with gene expression analysis, indicated that *At*FAD7 is the major ω-3 desaturase either in leaves or in non-photosynthetic tissues like roots, when compared to *At*FAD8. Relative abundance of both *At*FAD7 and *At*FAD8 proteins was analysed in response to wounding,

temperature or hormones like JA and ABA and a specific behaviour of both proteins was observed. In most cases, a positive correlation between transcript and protein levels could be stablished, suggesting that transcriptional control is at the basis of their coordination. Finally, bimolecular fluorescence complementation (BiFC) analysis using both FAD7 and FAD8 ω-3 desaturases with the ω-6 desaturase FAD6, responsible of 18:2 biosynthesis in the plastid, indicated that FAD7 and FAD8 interacted with FAD6 *in vivo*, but not among them, at least significantly. These results suggested the existence of supramolecular complexes involved in the production of TAs within plastid membranes.



## Results

### Generation of transgenic lines expressing *At*FAD7 and *At*FAD8 proteins fused to GFP under the control of their endogenous promoters.

A strategy based in the use of protein fusions to GFP expressed under the control of the endogenous promoters of both genes was developed to analyse *At*FAD7 and *At*FAD8 at the protein level. First, two sequences of 1682 and 2958 bp upstream of the *AtFAD7* and *AtFAD8* ATG codons, respectively, were chosen to be analysed for their promoter activity. The 1682 bp upstream sequence of the *AtFAD7* (*At3g11170*) gene, located at chromosome 3, contained 853 bp of the non-coding sequence upstream the *AtFAD7* gene and 843 bp of the coding sequence of the *At3g11165* gene, located in the antisense strand, that encodes a protein with unknown function according to TAIR (Supplementary Fig. 1). In the case of the *AtFAD8* gene (*At5g05580*), the 2958 sequence upstream its ATG was located in chromosome 5 and contained 438 bp corresponding to the non-coding upstream sequence from the *AtFAD8* gene and 2520 bp of the coding sequence of the *At5g05570* gene, located in the same strand than *AtFAD*8

(Supplementary Fig. 1). *At5g05570* encodes a nuclear transducing protein with methyl-transferase activity, according to TAIR. Election of these long sequences was made after analysis with PLACE (https://sogo.dna.affrc.go.jp/cgi-bin/sogo.cgi?lang=en&pj=640&action=page&page=newplace) and PlantCARE (http://bioinformatics.psb.ugent.be/webtools/plantcare/html/) tools, which located several putative regulatory elements in these upstream sequences from both promoters that could be involved in their specific regulation (Supplementary Fig. 1). Prior to their utilization for protein analysis, these promoter sequences were fused to GUS to check for promoter activity. Several independent T3 lines carrying the 1,7 kb *AtFAD7* promoter fused to GUS (*AtFAD7*p1,7kb:GUS) were analyzed by GUS staining. High GUS activity was detected upon 1 h staining on leaf tissue including vasculature in either cotyledonal or rosette leaves from 14-day-old plants grown in control conditions (Fig. 1A and 1B). GUS staining was also detected in either primary or secondary roots, concretely in root vasculature as well as in the root tip (Fig.1C). No GUS staining was detected in leaves or roots from transgenic lines expressing the empty pMDC163 vector (Fig.1J-L). In independent T3 lines harboring the *AtFAD8* gene putative promoter (*AtFAD8*p3kb::GUS), 1 h staining only produced significant GUS activity in cotyledonal leaves (Fig. 1D-F). When the time of staining was increased up to 3 h, GUS activity was high in cotyledonal leaves and could also be detected in rosette leaves from 14-day old plants (Fig.1G and H), but with much lower intensity than that of the *AtFAD7*p1.7kb::GUS lines after 1 h. In the *AtFAD8*p3kb::GUS lines, very low GUS staining was detected in roots (Fig. 1K).

In order to confirm these results, those lines which showed a reproducible pattern of GUS staining, were selected for the determination of GUS activity. To that end, either leaf or root extracts were obtained from several independent transgenic lines. As shown in Fig. 1M, leaf extracts from transgenic lines carrying the *AtFAD7* 1.7 kb promoter sequence showed a

glucuronidase activity with values that ranged from 20 to 25 nmol MUG. $min^{-1}$ mg. $protein^{-1}$. These MUG activity values were very similar to those reported previously by Nishiuchi et al., (1995) when they assayed an Arabidopsis 824 bp *FAD7* promoter fragment in transgenic tobacco lines. Plants carrying the 3 kb *AtFAD8* promoter fragment showed reduced levels of GUS activity when compared with those carrying the 1.7 kb *AtFAD7* promoter fragment, with values between 4-5 nmol MUG. $min^{-1}$ mg. $protein^{-1}$ (Fig. 1M). These differences in promoter activity were consistent with the differences in GUS staining time required for GUS activity detection in both promoters. GUS activity was also monitored in root extracts from these transgenic lines. Root extracts from transgenic lines carrying the *AtFAD7* 1.7 kb promoter sequence showed values lower than 2 nmol MUG. $min^{-1}$ mg. $protein^{-1}$; much lower than those detected in leaves. GUS activity in roots from plants carrying the 3 kb *AtFAD8* promoter fragment was barely undetectable under our experimental conditions.

Once the activity of both *AtFAD7* and *AtFAD*8 gene promoter sequences was analysed, transgenic lines were obtained that expressed the *At*FAD7-GFP fusion under the control of the 1,7 kb *AtFAD7* promoter (designated as TG7 lines) and lines expressing the *At*FAD8-GFP fusion under the control of the 3 kb *AtFAD8* promoter (designated as TG8 lines). We first analysed the expression of both *AtFAD7* and *AtFAD8* genes in these transgenic lines compared to that from the Col0 line. A group of lines was selected that showed increased *AtFAD7* or *AtFAD8* mRNA levels compared to Col0, consistent with the expression of the endogenous *AtFAD7* or *AtFAD8* genes in the Col0 background. Thus, TG7 lines showed an average increase in *AtFAD7* transcript levels of 2-3 fold with respect to Col0 lines while *AtFAD8* gene expression was comparable to that from Col0 (supplementary Fig. 2A). Similarly, TG8 lines showed an average increase in *AtFAD8* transcript levels of 2-fold, with respect to Col0 lines without significant changes in *AtFAD7* transcript levels (supplementary Fig. 2A). These results suggested that the transgene did not significantly affect to the expression of the other ω-3

plastidial desaturase counterpart gene. This was also confirmed by the analysis of the expression of the reticular ω-3 desaturase *AtFAD3* in either Col0, TG7 and TG8 lines, with no changes in *AtFAD3* transcript levels (supplementary Fig. 2A). The phenotype of the selected TG7 and TG8 plants was also analysed. Essentially, no differences in growth, leaf or rosette size or flowering pattern were detected in TG7 or TG8 lines when grown under control culture conditions (supplementary Fig. 2B).

**Confocal microscopy analysis of *At*FAD7-GFP and *At*FAD8-GFP protein distribution in TG7 and TG8 lines.**

Confocal microscopy analysis of transgenic lines expressing *At*FAD7-GFP or *At*FAD8-GFP fusions, under the control of their respective endogenous promoters, is shown in Fig. 2. 14 day-old TG7 transgenic lines showed a strong GFP signal associated with chloroplasts from either cotyledonal or rosette leaves. In all cases, the GFP fluorescent signal was detected as a typical ring covering the whole plastid surface that fully co-localized with the chlorophyll red auto-fluorescence, indicating that the signal was plastid specific (Figs. 2A-C). It is worth mentioning that the signal was strongly detected in plastids from both young (Fig. 2B) and mature rosette leaves (Fig. 2C), being less abundant in cotyledonal leaves (Fig. 2A). In young rosette leaves and to a lesser extent in mature rosette leaves, a strong GFP signal was also detected in small chloroplasts (Figs. 2B and 2C). When TG8 transgenic lines were analysed, low GFP fluorescent signal was observed in plastids from cotyledonal or rosette leaves (Fig. 2D-F). No GFP signal associated with small chloroplasts was detected in TG8 plants. Transgenic plants carrying the empty vector (pEN-R2F-L3) did not show any GFP fluorescent signal, detecting only the chlorophyll red auto-fluorescence signal from plastids (Supplementary Fig. 3). These results suggested that the FAD7 protein was much more abundant than FAD8 in Arabidopsis leaves.

Omega-3 fatty acids (18:3 and 16:3) are less abundant in roots, with an average mole percent of 24.6% and 1.56% of 18:3 and 16:3, respectively, in 15 day-old roots (Beaudoin et al., 2009; Miquel and Browse, 1992). In spite of this lower TA content, the FAD7 protein was detected in roots from TG7 lines. The distribution of the fluorescent GFP signal in root tissues was not homogeneous. Strong GFP fluorescent signal was detected in the root-tip (Fig. 3A) and in the cells surrounding the root vasculature (Fig. 3D), consistent with the GUS-staining data. In TG8 lines, the GFP signal was detected in the cells surrounding the root vasculature (Fig. 3E). Almost no GFP signal, if any, was detected in the root-tip (Fig. 3B). Transgenic lines expressing the empty pEN-R2F-L3 vector showed only the red fluorescence signal associated with the propidium-iodide staining (Fig. 3C and 3F), indicating that the GFP signal detected in the root, mostly with the FAD7 construct, was specific. Since light has been reported as a regulatory signal for FAD7 gene expression (Nishiuchi et al., 1995; Collados et al., 2006), we analysed whether the presence of the *At*FAD7 protein in the root could be caused by illumination of the root tissue. To that end, TG7 plants were grown vertically in MS plates with the area of root growth covered to avoid illumination. Confocal microscopy analysis of covered roots from TG7 plants showed a similar pattern of FAD7 localization when compared to fully illuminated plants (Supplementary Fig. 4), indicating that the presence of the *At*FAD7 protein in the root was not an artefact of illumination.



**Relative abundance of the *At*FAD7 and *At*FAD8 proteins in leaf and root tissues**

Relative protein abundance was analyzed by western blot, using an anti-GFP antibody, to confirm the confocal microscopy data. Protein extracts were obtained from rosette leaves and roots from 14 day-old TG7 and TG8 transgenic lines. A band of 70-78 kDa molecular weight was detected in protein extracts obtained from rosette leaves of TG7 plants (Fig. 4, left panel). The apparent size of this band (around 70 kDa) was consistent with the molecular weight of the

FAD7 protein (50 kDa) and that of GFP (27 kDa). The 70 kDa band representing the FAD7-GFP monomer was highly abundant in extracts from leaves of TG7 plants. A strong signal in the high molecular weight range (> 100 kDa) was also detected repeatedly in the western blot analysis (Fig. 4), which could be originated by protein aggregates, usual in membrane proteins like FAD7. In addition, several faint bands in the low molecular range (< 30 kDa) were also detected (Fig. 4) that may represent degraded GFP protein. In the case of the *At*FAD8 protein, a band with a molecular weight around 70 kDa, compatible with that of the FAD8 protein (50 kDa) fused to GFP (27 kDa), was detected (Fig. 4, left panel). The bands detected in both TG7 and TG8 had a similar molecular weight consistent with the almost identical deduced molecular mass of *At*FAD7 and *At*FAD8 proteins. These results indicated that, although in lower amounts, *At*FAD8 was present in leaf protein extracts at control temperatures. Nevertheless, these data confirmed that the *At*FAD7 protein is the major ω-3 desaturase in leaves. The FAD7-GFP protein was also detected in roots from TG7 lines, but at much lower amounts than those detected in leaves (Fig. 4, right panel). No FAD8-GFP protein was detected in root extracts from TG8 lines (Supplementary Fig. 5), indicating that, as occurred in leaves, *At*FAD7 was also the major plastidial ω-3 desaturase in root tissues.

To further investigate the role of plastidial ω-3 desturases, particularly FAD7, in roots, several mutants deficient in fatty acid desaturase activity were grown in MS agar plates for 10 days and fatty acid composition of total root lipids was determined. These mutants included a *fad3-1* mutant, deficient in FAD3 activity (Browse et al., 1993); two T-DNA insertion lines in the *FAD7* and *FAD8* genes, *fad7i* and *fad8i* (Román et al., 2015) and a *fad7-2 fad8-1* double mutant (McConn et al., 1994). Col-0 plants showed a 19,5% of 18:3 fatty acids, with a high content of 18:2 (25,5%) and 16:0 (20%) as major fatty acids in roots (Table 1). This fatty acid composition is consistent with that reported previously for Arabidopsis root total lipids (Li-Beisson et al., 2013). The *fad3-1* mutant showed a dramatic decrease to 4.16% of 18:3 in its root lipids and a

concomitant increase of 18:2 levels up to 45% (Table 1). On the contrary, all mutations affecting plastidial ω-3 desaturases showed no reduction of 18:3 content in root lipids, with almost similar or even slightly higher levels of 18:3 (Table 1). These results further confirmed that the major desaturase responsible of TA biosynthesis in roots is FAD3. In spite of the fact that the FAD7 plastidial desturase was detected in roots, it seemed not to be essential for TA synthesis.

**Relative abundance of leaf *At*FAD7 and *At*FAD8 proteins in response to wounding and hormones**

The effect of wounding and jasmonate supplementation on *At*FAD7 and *At*FAD8 protein levels was studied. First, the expression of both *AtFAD7* and *AtFAD8* genes was monitored in Col-0, TG7 and TG8 plants after wounding or 100 μM MeJA treatment for 1 and 2h, to correlate transcript levels with changes in protein abundance. LOX2 was used as internal control of the MeJA treatment (Supplementary Fig. 6). RT-qPCR expression analysis showed that in Col0 *AtFAD7* mRNA increased up to 4-fold upon 1 h wounding with respect to control-unwounded Col0 plants (Fig. 5A). These high *AtFAD7* mRNA levels were maintained after 2 h of wounding (Fig. 5A). A similar increase of *AtFAD7* mRNA levels upon wounding was also detected in TG7 or TG8 lines (Fig. 5A). This response of the *AtFAD7* gene seemed to be specific since no changes were detected for the *AtFAD8* mRNA upon wounding in either Col0, TG7 or TG8 lines. Exposure of Col0 plants to MeJA resulted in an average 1.7-fold increase of *AtFAD7* mRNA with respect to Col0 untreated plants after 1 h of treatment, but increased up to 3,5-fold after 2h of MeJA exposure (Fig. 5A). TG7 lines also experienced a high increase of *AtFAD7* mRNA upon JA treatment, reaching average values of 5,5 fold with respect to control untreated TG7 plants (Fig. 5). This increase was also observed in TG8 lines, which showed an expression pattern of *AtFAD7* gene upon wounding almost similar to that from Col0 plants (Fig. 5).

Differently to what happened upon wounding, JA treatment also modified the expression of the *AtFAD8* gene. Thus, Col0 plants showed an increase of *AtFAD8* transcript levels that reached on average 2-fold values after 2 h of treatment (Fig. 5A). Similar increases were also detected in either TG7 or TG8 lines, suggesting that MeJA induced *AtFAD8* gene expression.

We correlated the changes in transcript levels with changes in protein levels. To that end, mature 14 day-old Arabidopsis TG7 and TG8 plants were subjected to wound treatment by pressing the leaf with forceps. Leaves were flash frozen at 1 and 2 h after wounding, protein extracts were obtained and analyzed by western blot, using GFP antibodies. Total amount of protein extract was increased to 30-35 µg in the TG8 lines to favour its detection in the view of the previous data (Figs. 1 and 2). *At*FAD7 protein levels increased upon wounding in TG7 plants (Fig. 5B). This increase in *AtFAD7* protein levels could be correlated with changes in *At*FAD7 transcript levels in TG7 plants upon wounding (Fig. 5A). TG8 lines did not show any changes in *At*FAD8 protein levels upon wounding (Fig. 5B), consistent with the gene expression data and indicating that *At*FAD8 was not sensitive to wounding neither at the gene or protein levels. JA supplementation was also investigated. TG7 and TG8 lines were sprayed with a 100 µM MeJA solution. Rosette leaves were taken at 1 h and 2 h after MeJA treatment, protein extracts were obtained and western blot was carried out using the anti-GFP antibody. JA supplementation did not result in significant changes of the *At*FAD7 protein levels in TG7 plants (Fig. 5B). On the contrary, an increase in *At*FAD8 protein levels was observed upon 1 h of MeJA supplementation in TG8 lines (Fig. 5B). This increase was consistent with the qPCR expression data, suggesting that *At*FAD8 was JA-sensitive wound-independent.

Abscisic acid (ABA) is the major hormone involved in plant responses against abiotic stresses like drought, salt or cold (reviewed in Zhu, 2002). We investigated the effect of ABA on the relative abundance of both *At*FAD7 and *At*FAD8 proteins. Again, expression analysis of both *AtFAD7* and *AtFAD*8 genes in Col0, TG7 and TG8 plants in response to ABA was carried out.

ABI1 was used as internal control of the ABA treatment (Supplementary Fig. 6). Addition of ABA to Col0 plants resulted in a strong decrease (more than 50% with respect to control values) of the *AtFAD7* mRNA in leaves with respect to Col0 untreated plants (Fig. 6A). A similar decrease was detected in TG7 or TG8 plants (Fig. 6A). This effect of ABA was specific of *AtFAD7* since no significant modifications of *AtFAD8* mRNA levels were observed in leaves upon ABA addition in Col0, TG7 or TG8 plants (Fig. 5A). The effect of ABA was also monitored at the protein level. Both TG7 and TG8 plants grown in MS plates were subjected to 100 µM ABA treatment for 48 h and then western blot analyses using the anti-GFP antibody was performed. As shown in Fig. 6B, ABA treatment resulted in a dramatic decrease of *At*FAD7-GFP protein in TG7 plants. On the contrary, no changes in *At*FAD8-GFP protein levels were observed in TG8 lines, indicating that the effect of ABA was specific of *At*FAD7 and seemed to operate both at the transcript and protein levels. Confocal microscopy of TG7 plant lines was performed to contrast the results obtained by western blotting. As shown in Supplementary Fig. 5, TG7 lines treated with 100 µM ABA for 48 h showed a dramatic decrease of the GFP fluorescent signal when compared with untreated control plants, indicating that ABA specifically affected *AtFAD7* gene expression in Arabidopsis leaves.

**Effect of temperature on *At*FAD7 and *At*FAD8 protein levels**

The effect of low (6 ºC) or high (35 ºC) temperatures on *At*FAD7 and *At*FAD8 protein levels was also investigated. When cold temperatures were analysed, 14 day-old Col0, TG7 and TG8 plants were kept at 6 ºC for an additional week. Then rosette leaves were frozen for further mRNA and protein analysis. As shown in Fig. 7A, *AtFAD7* mRNA levels decreased in Col0 plants upon exposure to cold temperatures. This decrease is consistent with previous data in Arabidopsis or maize (Román et al., 2015; Berberich et al., 1998). However, no changes in *AtFAD7* transcript levels were detected in TG7 or TG8 lines upon cold temperature exposure

(Fig. 7A). On the contrary, *AtFAD8* mRNA showed an increase of 2-fold in Col0, TG7 and TG8 plants upon cold temperature exposure (Fig. 7A), consistent with previous observations in Arabidopsis (McConn et al., 1994; Román et al, 2015). Then, total leaf protein extracts from TG7 and TG8 plant lines grown at 22 ºC or kept at 6 ºC for an additional week were obtained and blotted with the anti-GFP antibody. OEE33 was used as internal control. As shown in Fig. 7B, TG7 lines showed no changes in *At*FAD7-GFP protein levels upon exposure to 6 ºC. Conversely, TG8 lines showed a clear increase of the *At*FAD8-GFP protein levels (Fig. 7B), which correlated with the changes in *AtFAD8* mRNA in response to cold (McConn et al, 1994; Román et al., 2015). Confocal microscopy analysis was performed to contrast the western blot protein data. TG8 plants showed an increase in GFP fluorescence associated to the *At*FAD8 protein at low temperatures (Supplementary Fig. 7A). This increase was specific since no changes were observed in TG7 plants (Supplementary Fig. 7A). These results confirmed the western blot analysis and indicated that cold temperatures affected to the *AtFAD8* gene both at the transcriptional and protein levels.

The effect of high temperatures was also studied. To that end, 2 week-old Col0, TG7 and TG8 plants were exposed to 35 ºC for 5 days. Then, rosette leaves were frozen and kept for further analysis. Col0 plants showed a decrease of *AtFAD7* mRNA levels upon high temperature exposure, reaching values closer to 50% those of control untreated plants (Fig. 7A). However, this decrease in *AtFAD7* mRNA levels was not observed in TG7 or TG8 plant lines (Fig. 7A). When the expression of *AtFAD8* gene was analyzed, no changes in transcript levels were detected in Col0, TG7 or TG8 plants upon 35 ºC treatment (Fig.7A), suggesting that high temperature exposure did not affect to the *AtFAD8* gene at the transcriptional level. Then, changes in protein abundance were also analyzed. *At*FAD7-GFP protein levels did not show any significant change upon exposure of plants to 35ºC for 5 days (Fig. 7B). On the contrary, TG8 lines showed a dramatic decrease of *At*FAD8-GFP protein levels upon exposure to high

temperatures (Fig. 7B). This decrease might be consistent with previous observations in Arabidopsis using chimeric myc-FAD8 fusions (Matsuda et al., 2005). These results suggested that *At*FAD8 was highly sensitive to temperature and that high temperatures affected its expression at the post-transcriptional level.

**Analysis of the *in vivo* interaction of plastidial ω-3 desaturases with the plastidial ω-6 desaturase FAD6**

We analyzed whether both plastidial ω-3 desaturases FAD7 and FAD8 can interact *in vivo* with their plastidial counterpart, the ω-6 desaturase FAD6. To that end, a bimolecular fluorescence complementation assay (BiFC) using the split-YFP system in Arabidopsis protoplasts was performed. The different constructs carrying each desaturase (FAD6, FAD7 or FAD8) were co-transformed in protoplasts and the interactions between pairs of proteins were monitored by the detection of the YFP signal. The BiFC analysis showed the existence of interactions between the ω-6 FAD6 and the ω-3 FAD7 desaturases, obtaining similar results when both proteins carried either the N-terminus or C-terminus portion of the YFP (Fig. 8C and D). When the interaction between FAD6 and FAD8 was tested, the YFP signal was detected with both protein pairs, although the data showed better results when the FAD6 protein carried the N-terminus of the YFP protein and FAD8 the C-terminus of the YFP (Fig. 8E and F). Since the YFP signal is not only dependent of the distance but also the orientation of both proteins, these results might suggest some preference of certain regions from both proteins for the interaction.

The possibility of forming heterodimers between FAD7 and FAD8 ω-3 desaturases was also tested. Very weak YFP signal was obtained when the FAD7/FAD8 protein pair was assayed (Fig. 7G and 7H), suggesting that, if it occurs; this interaction might be very weak. On the contrary, both ω-3 desaturases could form homodimers *in vivo* as deduced from the results

obtained when the assay was performed with the FAD7 or FAD8 proteins, respectively (Fig. 7I and 7J).

In parallel, we performed a co-localization analysis of ω-3 and ω-6 desaturases in the plastid. To that end, both plastidial ω-3 desaturases *At*FAD7 and *At*FAD8 were fused to YFP and expressed under a constitutive 35S promoter. The plastidial ω-6 desaturase *At*FAD6 was fused to CFP under the control of a constitutive 35S promoter. Then, transient expression experiments were performed on *N. benthamiana* leaves in which the 35S:FAD7-YFP or 35S:FAD8-YFP were co-transformed with the 35S:FAD6-CFP construct. Confocal microscopy of transiently transformed N. benthamiana leaves was performed. Special care was taken to confirm that no YFP signal was detected through the CFP channel and viceversa under our experimental conditions. As shown in Supplementary Fig. 8, FAD7 and FAD8-YFP signals were detected in the chloroplasts from *N. benthamiana*. They were detected as a yellow signal associated with chlorophyll autofluorescence (Fig. S8). Intense yellow fluorescence dots or *foci* were also detected for both proteins. This pattern of localization in discrete *foci* is shared with many plastid proteins, particularly those located in the envelope, expressed under constitutive promoters (Breuers et al., 2012). We have already described such a pattern for *At*FAD7, *At*FAD8 and Tic40 proteins (Roman et al., 2015). FAD6-CFP protein was also detected although with less intensity that the yellow ones (Fig. S8). Interestingly, when both FAD7-YFP/FAD8YFP and FAD6-CFP signals were merged, most of the signal seemed to overlap (Fig. S8), suggesting that ω-3 and ω-6 plastid desaturases are located in close vicinity in the membrane, consistent with the BiFC analysis.

## Discussion

In this work, we analysed the non-redundant role of the ω-3 plastidial desaturases *At*FAD7 and *At*FAD8 in response to stress and hormones. We analysed the transcriptional and post-transcriptional components of their differential regulation, and their relative abundance and protein distribution in several plant tissues. To that end, stable transgenic lines that expressed both *At*FAD7 and *At*FAD8 proteins fused to GFP under the control of their endogenous promoters were used. Our expression analysis by qRT-PCR and GUS staining and activity, as well as confocal microscopy and western blot data showed that, under normal growth conditions, the *At*FAD7 protein was highly abundant in leaves and detected in lower amounts in roots. The analysis of *AtFAD8*p3kb::*FAD8-GFP* (TG8) lines showed that *At*FAD8 protein was present in leaves from plants grown at 22 ºC, but at much lower amounts than *At*FAD7, indicating that FAD7 was the major ω-3 desaturase in the plastid. This higher abundance of FAD7, particularly in leaf tissue, is consistent with its higher promoter activity and the higher specificity of FAD7 for galactolipids MGDG and DGDG, which are the major chloroplast lipids with higher TA content. The lower relative abundance of *At*FAD8 could be also explained by its lower promoter activity, as shown in the GUS data. *At*FAD8 has higher specificity for PG or sulpholipids (Román et al., 2015), which are minor components of leaf plastid membranes (around 5%). These results suggest that transcriptional control is key to determine the differences in relative abundance between both proteins at least in leaves.

Our data showed that the *AtFAD7* gene was expressed and the *At*FAD7 protein accumulated in roots. Root lipids do not contain high levels of TAs, being FAD3 the major contributor to their synthesis in this tissue (Lemieux et al., 1990; Table 1). Furthermore, MGDG and DGDG are very minor components of root lipids (less than 5%; Li-Beisson et al., 2013) and can be originated in the RE in form of PC, desatured by FAD3 and later transported to the plastid in form of DAG. This DAG could be converted to 18:3 MGDG or DGDG in the plastid. This

might help to explain how 18:3 is synthetized in the absence of reduced ferredoxin, since cytochrome $b_5$ is the electron donor of FAD3. On the other hand, although we did not detect 16:3 in our analysis, others (Beaudoin et al., 2009) detected a 1,5 % of 16:3 in total lipids from roots. This very minor 16:3 could only be originated from the activity of *At*FAD7. However, other roles cannot be discarded. Thus, both our GUS-staining data as well as the confocal microscopy localization analysis show a specific distribution in the root tip and adjacent to the root vasculature (Figs. 1 and 3). This distribution is similar to that of some genes involved in JA biosynthesis or signalling like LOX9 (Hayashi et al., 2008) or JAZ1 (Meesters et al., 2014). These results open the possibility that the role of *At*FAD7 in roots might be more related with JA biosynthesis than the mere TA biosynthesis for membrane lipids.

Our data point to the existence of specific and highly coordinated responses of *At*FAD7 and *At*FAD8 desaturases to stress and hormones. Thus, *At*FAD7, but not *At*FAD8 protein increased in response to wounding, consistent with the gene expression analysis (Fig. 5). Given the position of *At*FAD7 at the start of the jasmonate biosynthetic pathway providing precursors (TAs) for its synthesis, this wound-responsive behaviour is not striking. However, no changes in *At*FAD7 protein were detected in response to JA even when an increase in *AtFAD7* mRNA levels was observed (Fig. 5). On the contrary, *At*FAD8 showed a clear JA-dependent response both at the gene expression and protein levels (Fig.5). These results suggest that both plastidial desaturases are coordinated in defence responses in a specific manner, showing differences in their wound and JA-dependent profile. Such differences have been already described for many wound- and JA- responsive genes through different studies, including microarray analysis (Titarenko et al., 1997; Howe, 2004; Taki et al., 2005). It has been proposed that two signalling pathways are activated upon wounding: one might be responsible of the activation of the defence response at the wound site (local) independent of JA, while the other one involves JA perception and biosynthesis to activate and sustain the defence response in the rest of the plant

(systemic response), Howe (2004). *At*FAD7 and *At*FAD8 proteins might differently participate in these two wounding signalling pathways. Furthermore, differences in defence responses against herbivorous insects or necrotrophic pathogens have been reported in which JA-dependent and independent signalling pathways trigger different coordinated responses (Wasternack and Hause, 2013). It is tempting to speculate that the differences in wound and jasmonate response among *At*FAD7 and *At*FAD8 plastidial desaturases could be related with different sensitivity to insects or pathogen attack. More striking was the effect of ABA on FAD7 protein abundance. Both western blot and confocal microscopy analyses showed a dramatic decrease of *At*FAD7 protein levels in response to ABA (Fig. 6). This decrease occurred concomitantly with a decrease of *AtFAD7* mRNA levels (Fig. 6). This could be consistent with the presence of two ABA repression sequences, CAACTTG and GAAGTTG (Wang et al., 2011) placed at -278/-267 and -203/-197, respectively, with respect to the ATG in the *AtFAD7* promoter sequence (Fig. S1). These sequences are present in most ABA-repressed genes (Wang et al., 2011) and absent in *AtFAD8*. Since ABA is the major hormone involved in abiotic stress, this repression of *AtFAD7* gene expression and protein levels by ABA might be related with a higher specialization of FAD7 on biotic and defence responses (as supplier of JA biosynthesis precursors), that could be blocked antagonically by ABA. In that sense, our data also showed an increase of *AtFAD8* mRNA (Román et al., 2015) and protein levels in response to cold. The cold-specific response of *At*FAD8 might be consistent with its specificity for PG, and the specific role of this lipid in maintaining the stability of photosynthetic complexes under stress conditions (Wada and Murata, 2007). Our data also showed that *At*FAD8 was not sensitive to ABA neither at the gene nor protein levels (Fig.6). The different effect of cold, wounding, ABA or JA on the expression of *At*FAD7 and *At*FAD8 further demonstrates the non-redundant role of both plastidial ω-3 desaturases and the tight coordination of their activity in response to biotic and abiotic stresses. It is worth mentioning that, with the exception of the increase of *At*FAD7

mRNA upon JA supplementation, the increase (or decrease) in FAD7 or FAD8 protein levels, followed the increase (or decrease) of *AtFAD7* and *AtFAD8* transcript levels. These results suggest that transcriptional regulation is crucial for the control of plastidial ω-3 FAD7 and FAD8 desaturase activity and it is at the basis of the coordination of both ω-3 desaturases to stress and hormones. Analysis of the promoters from both genes and identification of the different regulatory elements participating in their specific responses might help to clarify this point.

Our bimolecular fluorescence complementation assay indicated that both plastidial ω-3 desaturases FAD7 and FAD8 can form heretodimers *in vivo* with their plastidial counterpart, the ω-6 desaturase FAD6, responsible of the biosynthesis of 18:2 (or 16:2) in the plastid. These results are consistent with yeast complementation studies that suggested that the ER ω-3 and ω-6 desaturases, FAD2 and FAD3 also formed heterodimers that might facilitate metabolic channelling of 18:1 to produce 18:3 *in vivo* (Lou et al., 2014). These results altogether point to the existence of quaternary complexes within the membrane as responsible of the production of polyunsaturated fatty acids. This is not striking if we consider that the soluble stearoyl-ACP desaturase, FAB2, the only desaturase for which a three-dimensional structure is available, also forms homodimers in its functional form *in vivo* (Lindqvist et al., 1996). Furthermore, many enzymes involved in the biosynthesis or modification of fatty acids like the fatty acid synthase (FAS) in the plastid or the fatty acid elongase (FAE) are constituted of a complex of specialized membrane proteins (Somerville et al., 2000), indicating that the production and modification of fatty acids is associated to the formation of membrane quaternary complexes, as seems to be the case of plastidial ω-6 and ω-3 desaturases. Further studies might be required to investigate how the specific FAD6/FAD7 and FAD6/FAD8 complexes are formed and how they are distributed within the envelope membrane.

## Conclusions

Our strategy based in the obtention of transgenic lines expressing both *At*FAD7 and *At*FAD8 proteins, fused to GFP, under the control of their endogenous promoters, has provided a picture of the tissue specific distribution and relative abundance of both plastidial ω-3 desaturases in leaves and non-photosynthetic tissues like roots. Our data have revealed a specific and highly coordinated response of both proteins to defence, temperature and phytohormones. There is a clear specialization between both ω-3 desaturases and a strong coordination, mainly controlled at the transcriptional level, between stress and hormone signalling pathways for the control of their specific activities. Functional dissection of their promoters will help to clarify how this coordination takes place.

## Materials and Methods

### Plant materials

*Arabidopsis thaliana* Col0 ecotype was used as wild-type. The transgenic lines generated in this work were obtained from Col0 plants. The fatty acid desaturase mutants *fad3-1*, *fad7i*, *fad8i* and the double mutant *fad7-2 fad8-1* were available from NASC. The *fad7i* and *fad8i* mutants were T-DNA insertion lines characterized in previous works (Román et al., 2015). The EMS *fad3-1* and double *fad7-2 fad8-1* mutants have been characterized previously (McConn et al., 1994). Arabidopsis seeds were sterilized and germinated in MS medium or directly in pots. Seeds were vernalized for 3 days at 4 ºC and then moved to a growth chamber for 14 days. 14 day-old rosette leaves were frozen in liquid nitrogen and stored at –80 ºC until use. Growth conditions were light intensity of 100 µmol. $m^{-2}$. $s^{-1}$ in a 16/8 h light/dark photoperiod at 22/18 ºC and a relative humidity of 60/65%.

### Generation of *AtFAD7*p1.7kb::*FAD7-GFP* (TG7) and *AtFAD8*p3kb::*FAD8-GFP* (TG8) Arabidopsis lines

Arabidopsis genomic DNA was isolated by CTAB method. Fragments of -1682 and 2958 bp corresponding to the *AtFAD7* and *AtFAD8* putative promoter sequences, respectively, were amplified by PCR using Phusion High-Fidelity DNA Polymerase (Thermo) and cloned in a pENTR-D-TOPO vector. *AtFAD7* and *AtFAD8* promoter fragments, flanked by the appropriate *attL* sites, were subcloned in a pMDC163 plasmid (Curtiss and Grossnicklaus, 2003) through Gateway technology using LRclonaseII. Agrobacterium mediated transformation (GV3101 strain) of Arabidopsis plants was performed by floral dip (Clough and Bent, 1998). Positive transformants were selected for hygromycine resistance and genotyped by Phire® Plant direct PCR kit (Thermo). Homozygote T3 lines were fully segregated and multiple independent

transgenic events were used for the analysis of GUS activity. To create the promoter::protein-GFP constructs, the two -1682 and 2958 bp fragments corresponding to the *AtFAD7* and *AtFAD8* putative promoter sequences, respectively, were amplified by PCR using Phusion High-Fidelity DNA Polymerase lines and specific primers (Supplementary table 1) that contained *KpnI* and *XmaI* restriction sites to allow their cloning in the pUC57 L4-KpnI_XmaI-R1 vector. This introduced two attL4 and attR1 sequences flanking both promoters to facilitate their directional multisite gateway cloning into the entry vector. In parallel, pENTER D-TOPO vectors carrying the coding sequences from both *AtFAD7* and *AtFAD8* genes without their respective STOP codons were used (Román et al., 2015). A third plasmid, pEN-R2F-L3, (Plant Systems Biology, Ghent University, Belgium; Karimi et al., 2007) contained a GFP coding sequence flanked by two *attR2* and *attL3* sequences. Multisite gateway cloning was performed using the plasmid pH7m34GW (Plant Systems Biology, Ghent University, Belgium; Karimi et al., 2005) as destination vector and the enzyme LR Clonase II®. Positive transformants were selected in streptomycin/spectinomycin selective media and further checked by *KpnI*, *XmaI* digestion and sequencing of the positive selected clones. Positive Arabidopsis transformants were selected for hygromycine resistance and were genotyped by Phire® Plant Direct PCR Kit (Thermo). Homozygote lines T3 were segregated. Lines producing 100% resistant plantlets were selected (T3 homozygous lines, single insertion locus) and used for further analysis. Plants carrying the *AtFAD7*p1,7kb::*FAD7-GFP* were designated as TG7 lines while those carrying the *AtFAD8*p3kb::*FAD8-GFP* were designated as TG8 lines. In all the experiments, data from three independent transgenic events were used for the analysis.

**Histochemical and fluorimetric GUS assays**

GUS staining protocol was adapted from Jefferson et al, (1987). Samples were vacuum infiltrated for 15-20 min with GUS staining buffer (50 mM sodium phosphate, pH=7.2, 10 mM EDTA, 2.5 mM potassium ferricyanide, 2.5 mM potassium ferrocyanide, and 0.1% (v/v) Triton X-100) containing 1 mg/ml 5-bromo-4-chloro-3-indolylglucuronide (Thermo). GUS staining was performed at 37 ºC in darkness for 1-3 h. Chlorophyll was removed after 15 min EtOH:acetic acid (3:1 v/v) incubation and subsequent 70% EtOH (v/v) overnight incubation. Samples were visualized in a Leica M165 FC stereomicroscope. Results shown are representative of 3-6 individual plants of at least six transformation events. GUS fluorometric protocol was adapted from Vitha et al. (1993). Samples were homogenised in GUS extraction buffer (50 mM sodium phosphate, pH=7.2, 10 mM EDTA, 0.1% (v/v) Triton X-100, 0.1% (w/v) N-lauroylsarcosine sodium salt, and 0.7 µl/ml β-mercaptoethanol), and centrifuged at 14,000 x *g* for 5 min. Aliquots of the supernatants (100 µg protein) were assayed fluorometrically using 4-methyl-umbelliferyl-β-D-glucuronide as substrate. Fluorescence of aliquots was measured using a Synergy™ HT plate reader (BioTek) at 365 nm excitation and 455 nm emission wavelengths, respectively. Results shown are representative of at least three biological samples of at six independent transformation events.

**Experimental treatments**

For wounding treatments, 2 week-old Col0, TG7 and TG8 plants were wounded by pressing the leaf with forceps and kept in the growth chamber for 1 or 2 h. Wounded tissues were rapidly stored at –80 ºC. For low-temperature treatments, 2 week-old Col0, TG7 and TG8 plants were transferred to a 6-8 ºC bioclimatic chamber for an additional week, before being analyzed or stored at -80 ºC. For high-temperature experiments, 2 week-old Col0, TG7 and TG8 plants were

transferred to a growth chamber at 35 ºC for an additional week, before being analyzed or stored at -80 ºC. In both cases, some plants were kept at 20-22 ºC as control treatment. For ABA treatments, after one week of growth in MS plates, Col0, TG7 and TG8 plants were transferred to MS plates containing 100 µM (+/-)-abscisic acid (ABA, Sigma) for 48 h before being analyzed or stored at -80 ºC. For MeJA treatment, two-week old Col0, TG7 and TG8 plants were sprayed with 100 µM methyl jasmonate (MeJA, Sigma) for 1 or 2 h, before analyzed or stored at -80 ºC. ABA was dissolved in methanol and MeJA in water. Methanol and water were used for mock treatments in the hormone experiments. Analysis of variance (ANOVA) was applied to compare treatments. Statistical analyses was carried out with the program Statgraphics Plus for Windows 2.1, using a level of significance of 0.05.



**Quantitative PCR analysis**

Total RNA was extracted from 0.5 g of rosette leaves and 0.1 g of roots with Trizol (Life Technologies) according to manufacturer's instructions. First-strand cDNA was synthesized from 3 µg of DNAase-treated RNA with M-MLV reverse transcriptase (Promega) and oligo dT. Quantitative RT-PCR (qRT-PCR) was performed using a 7500 Real Time PCR System (Applied Biosystems), SYBR Green Master Mix (Applied Biosystems), and specific primers (Supplementary Table 1). The Ct values were calculated relative to EF1α reference gene (*At5g60390*) using $2^{-\Delta\Delta Ct}$ method (Livak and Schmittgen, 2001). Data were obtained from the analysis of at least three biological samples with three independent technical repeats for each sample.

**Confocal microscopy analysis**

Fresh leaf imaging was carried out on a Leica TCS SP2 confocal microscope (CIBA-IACS,

Zaragoza). Images were acquired using a 40x or 60x oil immersion objectives as described in Román et al., (2015). For root analysis, samples were incubated with 15 µM propidium iodide for 10 min in the dark and rinsed twice in water to stain the cell wall. Propidium iodide fluorescence was detected exciting with an Argon laser at 488 nm and emission was detected in the 600-680 nm range. Imaging of GFP emission was performed by sequential scanning. GFP was excited with a 488 line of an argon laser and the emission collected through a 505-560 nm emission filter. Autofluorescence of chlorophyll was excited with the 633 nm line of an argon laser, and the emission was collected through a 651-717 nm emission filter. Images were analyzed and merged using Leica AF and Image J software. In all cases, special care was taken to avoid overlapping of fluorescence signals.

For co-localization purposes, two constructs expressing both FAD7-YFP and FAD8-YFP proteins under the control of a constitutive 35S promoter were generated using pEarly101 as destination vector. A third 35S:FAD6-CFP construct was also generated using pEarly102 destination vector. Once available, these constructs were transformed individually in *Agrobacterium tumefaciens* (GV3101 strain). For co-localization, *N. benthamiana* leaves from 5-week old plants, grown at 22 ºC, 16 h light, 8 h dark photo period were infiltrated with a combination of *A. tumefaciens* cultures ($OD_{600nm}$ 0.5), harbouring either FAD7-YFP and FAD6-CFP or FAD8-YFP and FAD6-CFP. All constructs were co-infiltrated with the p19 plasmid to avoid silencing (Roman et al., 2015). Plants were kept in the growth chamber for 3-5 days before analysis. Imaging of YFP and CFP emissions were performed by sequential scanning. YFP and CFP were excited with a 514 and 458 nm line of an argon laser and the emission collected through a 518-580 nm emission filter for YFP and 465-500 nm for CFP. Autofluorescence of chlorophyll was excited with the 633 nm line of an argon laser, and the emission was collected through a 651-717 nm emission filter. Images were analyzed and merged using Leica AF and Image J software.

**Bimolecular Fluorescence Complementation (BiFC) Analysis**

Three fragments of 1341, 1308 and 1347 bp, respectively, corresponding to the coding sequences of *AtFAD7*, *AtFAD8* and *AtFAD6* genes (without their corresponding STOP codons) were amplified by RT-PCR using Phusion® High Fidelity polymerase. Primers used for amplification (Supplementary Table 1) contained two BamHI and XmaI restriction sites to facilitate their cloning in the corresponding vectors. pUC-SPYNE and PUC-SPYCE vectors (Walter et al., 2004), were used for the analysis. These vectors expressed the two target proteins fused to yellow fluorescent protein (YFP) in either N-terminal (pUC-SPYNE) or C-terminal (pUC-SPYCE) sites under the control of a 35S promoter. Protoplasts from Arabidopsis were obtained using the sandwich method (Wu et al., 2009) that uses Scotch® tape to remove the cuticle. Once the cuticle was removed with the tape, ten to fifteen leaves were incubated in a digestion mixture containing both Cellulase and Macerozyme (20 mM MES, pH: 5,7; 0.4 M Mannitol; 20 mM KCl; 10 mM $CaCl_2$; 1.5% (w/v) Cellulase and 0.4% (w/v) Macerozyme. Leaves were incubated in this mixture in darkness, at room temperature for no more than 1 h without agitation. Then, the mixture was diluted in washing buffer (20 mM MES, pH: 5,7; 125 mM $CaCl_2$; 5 mM KCl) and filtered through a 0,2 µm filter to eliminate debris and undigested material. Protoplasts were precipitated at 100 x *g* at 4 ºC for 5 min and carefully resuspended in a 15 mM MES, pH: 5,7; 0.4 M $MgCl_2$ solution. Integrity of the isolated protoplasts was analyzed in a Leica M165 FC stereomicroscope (Leica Microsystems).

Once isolated, protoplasts were transformed following the PEG/Ca method described by Yoo et al. (2007) with several modifications. The PEG percentage was adjusted to 30% to avoid protoplast lysis. For transformation, 100 µl of protoplasts and 100 µl of protoplast transformation solution (0.2 M mannitol, 100 mM $CaCl_2$, 30% (w/v) PEG4000) were mixed and 20 ng of DNA from each of the plasmids containing each of the protein pairs to be analyzed were added and incubated at room temperature for 20 min. The transformation reaction was

stopped by adding 400 µL of washing buffer and the protoplasts were precipitated by centrifugation at 100 x *g* at 4 ºC for 5 min. Protoplasts were carefully resuspended in 2 mL of a 4 mM MES pH: 5.7; 0.5 M KCl solution and kept under illumination at 22-24 ºC for 12-24 h before visualization of fluorescence. Fluorescence was detected with a Leica DM2500 fluorescence microscope using a 40x immersion objective. YFP fluorescence emission was detected with the YFP filter (excitation 500/20 nm; emission 535/30 nm). Chlorophyll auto-fluorescence was detected with the N2.1 filter (excitation 515/560 nm; emission 590 nm).



**Immunoblot analysis**

Protein extracts were obtained from 0.5 g of Arabidopsis rosette leaves or 0.1 g of roots homogenised in a mortar with liquid nitrogen. The powder was dissolved in buffer A (0.1 M Tris-HCl, pH: 7.5; 20% (w/v) glycerol, 1 mM EDTA; 10 mM $MgCl_2$, 14 mM β-mercaptoethanol, 100 µg/ml Pefabloc (Fluka), 1 µg/ml antipain (Sigma-Aldrich) and 1 µg/ml leupeptin, (Sigma-Aldrich) and filtered with Miracloth paper (Calbiochem). The protein content of the different fractions was estimated using the BioRad protein assay reagent (BioRad). Except when specifically mentioned, total protein of 20 µg was loaded per lane. Western blot procedures were performed as described in Román et al., (2015) using a GFP antibody (ab290, Abcam) at 1:1000 dilution. Anti-OEE33 (Alfonso et al., 2004), that recognizes the 33-kDa oxygen evolving extrinsic protein from Photosystem II, was used as an internal loading control (1:5000 dilution).

**Root lipid analysis**

Total lipids were obtained from 0.1 g of roots from plants of the different lines grown vertically in MS plates for two weeks, extracted as described (Bligh and Dyer, 1959) and analysed by gas

chromatography (GC), (Román et al., 2015). Data from fatty acid analysis were obtained from two independent biological experiments with two technical repeats per experiment. Analysis of variance (ANOVA) was applied to compare treatments with the program Statgraphics Plus for Windows 2.1, using a level of significance of 0.05.

## Funding

This work was supported by the Spanish Ministry of Economy and Competitiveness (MINECO, Grant AGL2014-55300-R) and Gobierno de Aragón, strategic research projects (A09-17-R). Á. S.-G. was recipient of a FPI fellowship from MINECO.

## Acknowledgements

We thank Dr. MV López (EEAD-CSIC) for assistance in the statistical analysis and P. Lorente and M. de la Vega for technical assistance.

## REFERENCES

Alfonso, M., Collados, R., Yruela, I, and Picorel, R. (2004). Photoinihibition and recovery in a herbicide-resustenta mutant from glycine max (L.) Merr cell cultures deficient in fatty acid unsaturation. *Planta* 291: 428-439.

Andreu, V., Lagunas, B., Collados, R., Picorel, R., and Alfonso, M. (2010). The *GmFAD7* gene family from soybean: identification of novel genes and tissue-specific conformations of the FAD7 enzyme involved in desaturase activity. *J. Exp. Bot.* 61: 3371-3384.

Berberich, T., Harada, M., Sugawara, K., Kodama, H., Iba, K., and Kusano, T. (1998) Two maize genes encoding ω-3 fatty-acid desaturase and their differential expression to temperature. *Plant Mol. Biol.* 36: 297-306.

Beaudoin, F., Wu, X., Li, F., Haslam, R.P., Markham, J.E., Zheng, H., Napier, J.A., and Kunst, L. (2009) Functional characterization of the Arabidopsis beta-ketoacyl-coenzyme A reductase candidates of the fatty acid elongase. *Plant Physiol.* 150: 1174–1191.

Bligh E. G, and Dyer W. S. (1959). A rapid method of total lipid extraction and purification. *Can. J. Biochem. Physiol.* 37: 911-917.

Bilyeu, K.D., Palavalli, L., Sleper, D.A., and Beuselinck, P.R. (2003) Three microsomal desaturase genes contribute to soybean linolenic acid levels. *Crop Sci.* 43: 1833-1838.

Breuers, F.K.H., Bräutigam, A., Geimer, S., Welzel, U.Y., Stefano, G., Renna, L., Brandizzi, F., and Weber, A.P.M. (2012) Dynamic remodelling of the plastid envelope membranes – atool for chloroplast envelope invivo localizations. *Front. Plant Sci.* 3: 1-10.

Browse, J., McCourt, P., and Somerville, C. (1986). A mutant of Arabidopsis deficient in C(18:3) and C(16:3) leaf lipids. *Plant Phys.* 81: 859-864.

Browse, J., McConn, M., James, D., and Miquel, M. (1993) Mutants o f Arabidopsis deficient in the synthesis of α-linolenate. *J. Biol. Chem.* 268: 16345-16351.

Collados, R., Andreu, V., Picorel, R., and Alfonso, M. (2006). A light-sensitive mechanism differently regulates transcription and transcript stability of omega-3 fatty acid desaturases (*FAD3*, *FAD7* and *FAD8*) in soybean photosynthetic cell suspensions. *FEBS lett.* 580: 4934-4940.

Clough, S.J., and Bent, A.F. (1998) Floral dip: a simplified method for *Agrobacterium*-mediated transformation of *Arabidopsis thaliana*. *Plant J.* 16: 735-743.

Curtis, M.D., and Grossnicklaus, U. (2003). A gateway cloning vector set for high-throughput functional analysis of genes *in planta*. *Plant Physiol.* 133: 462-469.

Dyer, J. M., and Mullen, R. T. (2001). Immunocytological localization of two plant fatty acid desaturases in the endoplasmic reticulum. *FEBS lett.* 494: 44-47.

Earley, K.W., Haag, R., Pontes, O., Opper, K., and Juehne, T. (2006). Gateway-compatible vectors for plant functional genomics and proteomics. *Plant J.* 45: 616-629.

Gibson, S., Arondel, V., Iba, K., and Somerville, C. (1994). Cloning of a temperature-regulated gene encoding a chloroplast omega-3 desaturase from *Arabidopsis thaliana*. *Plant Phys.* 106: 1615-1621.

Hamada, T., Nischiuchi, T., Kodama, H., Nishimura, M., and Iba, K. (1996) cDNA cloning of a wounding-inducible gene encoding a plastid omega-3 fatty acid desaturase from tobacco. *Plant Cell Physiol*. 37: 606-611.

Hayashi, S., Gresshoff, P.M., and Kinkema, M. (2008) Molecular Analysis of Lipoxygenases Associated with Nodule Development in Soybean. *Mol. Plant Microb. Int.* 21: 843-853.

Howe G. A. (2004) Jasmonates as signals in the wound response. *J. Plant Growth Regul.* 23: 223-237.

Iba, K. (2002) Acclimative response to temperature stress in higher plants: approaches of gene engineering for temperature tolerance. *Ann. Rev. Plant Biol.* 53: 225-245.

Jefferson, R.A., Kavanagh, T.A. and Bevan, M.W. (1987). GUS fusions: β-glucuronidase as a sensitive and versatile gene fusion marker in higher plants. *EMBO J.* 6: 3901 -3907.

Karimi, M., De Meyer, B. and Hilson, P. (2005) Modular cloning and expression of tagged fluorescent protein in plant cells. *Trends Plant Sci.* 10: 103-105.

Lagunas, B., Román, Á., Andreu, V., Picorel, R., and Alfonso, M. (2013). A temporal regulatory mechanism controls the different contribution of endoplasmic reticulum and plastidial ω-3 desaturases to trienoic fatty acid content during leaf development in soybean (Glycine max cv Volania). *Phytochemistry* 95: 158-167.

Lemieux, B., Miquel, M., Somerville, C., and Browse, J. (1990). Mutants of Arabidopsis with alterations in seed lipid fatty acid composition. *Theor. App. Gen.* 80: 234-240.

Li-Beisson, Y., Shorrosh, B., Beisson, F., Andersson, M.X. *et al*. (2013) Acyl-lipid metabolism. *Arabidopsis Book* 11: 161.

Lindqvist, V., Huang, W.S., Schneider, G., and Shanklin, J. (1996) Cristal structure of a Δ9 stearoyl-acyl carrier protein desaturase from castor seeds and its relationship to other diiron proteins. *EMBO J.* 15: 4081-4092.

Livak, K.J. and Schmittgen, T.D. (2001) Analysis of relative gene expression data using real-time PCR and the 2(-delta Delta C(T) method. *Methods* 25: 402-408.

Lou, Y, Schwender, J. and Shanklin, J. (2014) FAD2 and FAD3 desaturases from heterodimers that facilitate metabolite channeling *in vivo*. *J. Biol. Che*m. 289: 17996-18007.

Martz, F., Kiviniem,i S., Plava, T.E., and Sutinen, M.L. (2006). Contribution of omega-3 fatty acid desaturase and 3-ketoacyl-ACP synthase II (KASII) genes in the modulation of glycerolipid fatty acid composition during cold acclimation in birch leaves. *J. Exp. Bot.* 57: 897-909.

Matsuda, O., Sakamoto, H., Hashimoto, T., and Iba, K. (2005). A temperature-sensitive mechanism that regulates post-translational stability of a plastidial omega-3 fatty acid desaturase (FAD8) in Arabidopsis leaf tissues. *J. Biol. Chem.* 280: 3597-3604.

McConn, M., Hugly, S., Browse, J., and Somerville, C. (1994). A mutation at the FAD8 locus of Arabidopsis identifies a second chloroplast omega-3 desaturase. *Plant Phys*. 106: 1609-1614.

McConn, M. and Browse, J. (1996). The critical requirement for linolenic acid is pollen development, not photosynthesis in an Arabidopsis mutant. *Plant Cell* 8: 403-416.

Meesters, C., Mönig, T., Oeljeklaus, J., Krahn, D., Westfall, C.S., Hause, B., Jez, J.M., Kaiser, M., and Kombrink, E. (2014) A chemical inhibitor of jasmonate signaling targets JAR1 in *Arabidopsis thaliana. Nature Chem. Biol.* 10: 830–836.

Murata, N., Sato, N., Takahashi, N. and Hamazaki, Y. (1982). Compositions and positional distributions of fatty-acids in phospholipids from leaves of chilling sensitive and chilling resistant plants. *Plant & Cell Physiol.* 23: 1071-1079.

Nishida, I., and Murata, N. (1996). Chilling sensivity in plants and cyanobacteria: the crucial contribution of membrane lipids. *Ann. Rev. Plant Physiol. Plant Mol. Biol.* 47: 541-568.

Nishiuchi, T., Nakamura, T., Abe, T., T., Kodama, H., Nishimura, M. and Iba, K. (1995). Tisue specific and light-responsive regulation of the promoter region of the Arabidopsis thaliana chloroplast w-3 fatty acid desaturase gene (*FAD7*) *Plant Mol Biol.* 29: 599-609.

Nishiuchi, T., Hamada, T., Kodama, H., and Iba, K. (1997). Wounding changes the spatial expression pattern of the Arabidopsis plastid w-3 fatty acid desaturase gene (*FAD7*) through different signal transduction pathways. *Plant Cell* 9: 1701–1712.

Reymond, P., Weber, H., Diamond, M., and Farmer, E.E. (2000) Differential gene expression in response to mechanical wounding and insect feeding in Arabidopsis. *Plant Cell* 12: 707-719.

Román, A., Andreu, V., Hernández, M.L., Lagunas, B., Picorel, R., Martínez-Rivas, J.M., and Alfonso, M. (2012) Contribution of the different omega-3 fatty acid desaturase genes to the cold response in soybean. *J. Exp. Bot.* 63: 4973-4982.

Román, A., Hernández, M.L., Soria-García, A., López-Gomollón, S., Lagunas, B., Picorel, R., Martínez-Rivas, J.M., and Alfonso, M. (2015) Non-redundant contribution of the plastidial FAD8 omega-3 desaturase to glicerolipid unsaturation at different temperatures in *Arabidopsis*. *Mol. Plant* 8: 1599-1611.

Schaller, A. and Stinzi, A. (2009) Enzymes in jasmonate biosynthesis - Structure, function, regulation. *Phytochemistry* 70: 1532-1538.

Somerville, C., Browse, J., Jaworski, J.G. and Ohlrogge J.B. (2000). Lipids. In: Buchanan, B., Gruissem, W., Jones, R.L. (eds). *Biochemistry and Molecular Biology of Plants*. Am. Soc. Plant Physiol.. pp. 456-527.

Staswick, P.E., Su, W.P., and Howell, S.H. (1992). Methyl jasmonate inhibition of root growth and induction of a leaf protein are decreased in an *Arabidopsis thaliana* mutant. *Proc. Natl. Acad. Sci. USA.* 89: 6837-6840.

Taki, N., Sasaki-Sekimoto, Y., Obayashi, T., Kikuta, A., Kobayashi, K., Ainai, T., Yagi, K., Sakurai, N., Suzuki, H., Masuda, T., Takamiya, L., Shibata, D., Kobayashi, Y., and Ohta, H. (2005) 12-oxo-phytodienoic acid triggers expression of a distinct set of genes and plays a rrole in wound-induced gene expression in Arabidopsis. *Plant Physiol.* 139: 1268-1283.

Titarenko, E., Rojo, E., León, J., and Sánchez-serrano J.J. (1997) Jasmonic acid-dependent and -independent signaling pathways control wound induced gene activation in Arabidopsis thaliana. *Plant Physiol.* 115: 817-826.

Vitha, S., Benes, K., Michalova, M. and Ondrej, M. (1993) Quantitative β-glucuronidase assay in transgenic plants. *Biologia Plantarum* 35: 151-155.

Wada, H. and Murata, N. (2007). The essential role of phosphatidylglycerol in photosynthesis. *Photosynth Res.* 92**:** 205-215.

Walter, M., Chaban, C., Schutze, K., Batistic, O., Weckermann, K., Nake, C., Blazevic, D., Grefen, C., Schumacher, K., Oecking, C., Harter, K. and Kudla, J. (2004). Visualization of protein interactions in living plant cells using bimolecular fluorescence complementation. *Plant J.* 40: 428-438.

Wang, R.S., Pandey, S., Li, S., Gookin, T.E., Zhao, Z., Albert, R., and Assmann, S.M. (2011) Common and Unique elements of the ABA-regulated transcriptome of Arabidopsis guard cells. *BMC Genomics* 12: 216-240.

Wasternack, C. and Hause, B. (2013) Jasmonates: biosynthesis, perception, signal transduction and action in plant stress response, growth and development. An update to the 2007 review in *Annals of Botany*. *Ann. Bot*. 111: 1021-1058.

Wu, F. H., Shen, S. C., Lee, L. Y., Lee, S. H., Chan, M. T. and Lin, C. S. (2009). Tape-Arabidopsis Sandwich - a simpler Arabidopsis protoplast isolation method. *Plant Methods* 5: 16.

Yadav, N.S., Wierzbicki, A., Aegerter, M., Caster, C.S., Perez-Grau, L., Kinney, A.J., Hitz, W.D., Booth, R.J., Schweiger, B., Stecca, K.L., Allen, S.M., Blackwell, M., Reiter, R.S., Carlson, T.J., Russell, S.H., Feldmann, K.A., Pierce, J., and Browse, J. (1993) Cloning of higher plant ω3 fatty-acid desaturases. *Plant Physiol.* 103: 467-476.

Yoo, S. D., Cho, Y. H. and Sheen, J. (2007). Arabidopsis mesophyll protoplasts: a versatile cell system for transient gene expression analysis. *Nat Protoc*. 2: 1565-1572.

Zhu, J.K. (2002) Salt and drought stress signal transduction in plants. *Ann. Rev. Plant Biol*. 53: 247-273.

## FIGURE LEGENDS

**Figure 1**. Characterization of the *AtFAD7* and *AtFAD8* gene promoter sequences used in this work. GUS histochemical staining of transgenic lines carrying the 1682 bp sequence corresponding to the *AtFAD7* gene promoter after 1 h GUS-staining in cotyledonal leaves (A), rosette leaves (B), and roots (C). GUS histochemical staining of transgenic lines carrying the 2958 bp sequence corresponding to the *AtFAD8* gene promoter after 1 h (D-F) or 3 h (G-I) GUS-staining in cotyledonal leaves (D and G), rosette leaves (E and H), and roots (F and I). (J-L) plants carrying the pMDC163 empty vector. 14-d old rosette leaves and roots were used for the analysis. Bars are 200 µM (C, F, I and L) and 500µM (A-B, D-E, G-H and J-K). (M) GUS activity (nmol of 4-methylumbelliferone, MU) produced per minute per milligram of protein using 4-methylumbelliferyl β-D-glucuronide as a substrate. Each bar represnts the activity of an individual transgenic event. Data represent means of at least three biological replicates.

**Figure 2.** Localization of *At*FAD7 and *At*FAD8 proteins in leaves of TG7 (A-C) and TG8 (D-F) transgenic. Images show GFP and chlorophyll fluorescence in cotyledons (A and D), young rosette leaves (B and E), and mature rosette leaves (C and F) of two week-old plants. The localization in chloroplasts can be seen in the GFP images and in the merged images of the GFP and chlorophyll fluorescence channels. Bars correspond to 25 µm.

**Figure 3.** Localization of both *At*FAD7 and *At*FAD8 proteins in roots from TG7 (A-D) and TG8 (B and E) transgenic lines. Analysis was performed in roots from 2 week-old plants. Images show the overlay between the GFP (green) and propidium iodide (red) fluorescence channels in root tip (A-C) and root (D-F). Roots from empty vector plants (C and F). Bars correspond to 25 µm.

**Figure 4**. Western blot analysis of the relative abundance of *At*FAD7 and *At*FAD8 proteins in TG7 and TG8 transgenic lines. Protein extracts from 14 day-old rosette leaves from TG7 and TG8 transgenic lines (left panel). 20 µg of total protein were loaded per lane. AntiOEE33 was used as internal control. Protein extracts from roots and leaves of TG7 transgenic (right panel). 20 µg of total protein were loaded per lane. Anti-GFP was used as primary antibody. Total protein stained by Coomasie is shown as loading control.

**Figure 5**. Response of *At*FAD7 and *At*FAD8 to wounding and jasmonate. (A) qRT-PCR expression analysis of *AtFAD7* and *AtFAD8* genes in response to wounding (upper panel) or MeJA (lower panel) in Col0, TG7 and TG8 lines. Data represent means of at least three biological replicates. Asterisk indicates significant differences over than 2-fold or less than 0,5-fold related to the control. (B) Western blot analysis of the relative abundance of *At*FAD7 protein in TG7 and TG8 transgenic lines upon wounding (left panel) or 100 µM MeJA supplementation (right panel). For detection of the *At*FAD7-GFP protein 20 µg of total protein were loaded per lane. For detection of the *At*FAD8-GFP protein, 30-35 µg of total protein were loaded per lane. Anti-GFP was used as primary antibody. AntiOEE33 was used as internal control.

**Figure 6.** Effect of ABA on *AtFAD7* and *AtFAD8* gene expression and protein levels. (A) qRT-PCR expression analysis of *AtFAD7* and *AtFAD8* genes in response to 100 µM ABA treatment in Col0, TG7 and TG8 lines. Data represent means of at least three biological replicates. Asterisk indicates significant differences over than 2-fold or less than 0,5-fold related to the control. (B) Western blot analysis of the relative abundance of the *At*FAD7 and *At*FAD8 protein

in TG7 and TG8 lines in response to 100 µM ABA treatment. For detection of the *At*FAD7-GFP protein, 15-20 µg of total protein were loaded per lane. For the *At*FAD8-GFP protein, 30 µg of total protein were loaded per lane. AntiOEE33 was used as internal control.

**Figure 7**. Effect of cold or heat on *AtFAD7* and *AtFAD8* gene expression and protein levels. (A) qRT-PCR expression analysis of *AtFAD7* and *AtFAD8* genes in response to cold (6 ºC), (upper panel) or heat (35 ºC), (lower panel) in Col0, TG7 and TG8 lines. Data represent means of at least three biological replicates. Asterisk indicates significant differences over than 2-fold or less than 0,5-fold related to the control. (B) Western blot analysis of the relative abundance of the *At*FAD7 and *At*FAD8 protein in TG7 and TG8 lines at 22, 6 and 35 ºC. For detection of the *At*FAD7-GFP protein, 15-20 µg of total protein were loaded per lane. For the *At*FAD8-GFP protein, 30 µg of total protein were loaded per lane. AntiOEE33 was used as internal control.

**Figure 8.** Bimolecular fluorescence complementation analysis of the *in vivo* interaction of *At*FAD7 and *At*FAD8 proteins with the plastidial ω-6 desaturase *At*FAD6. All the red chlorophyll autofluorescence, yellow YFP and merged channels are shown for each pair. (A) protoplasts were transformed with a pEarley101 construct carrying the *At*FAD8 protein fused to YFP used as a positive control; (B) an empty pUC-SPYNE vector was used as negative control; (C) nYFP-FAD7/FAD6-cYFP pair; (D) nYFP-FAD6/FAD7-cYFP pair; (E) nYFP-FAD8/FAD6-cYFP pair; (F) nYFP-FAD6/FAD8-cYFP pair; (G) nYFP-FAD7/FAD8-cYFP pair; (H) nYFP-FAD8/FAD7-cYFP pair; (I) nYFP-FAD7/FAD7-cYFP pair; (J) nYFP-FAD8/FAD8-cYFP pair. Bars correspond to 100 µm.

**Supplementary Figure 1.** Schematic diagram of the constructs used for the analysis of the relative abundance of *At*FAD7 and *At*FAD8 proteins. Location of both *AtFAD7* and *AtFAD8* genes in chromosomes 3 and 5, respectively, is indicated. Position of genes upstream both *AtFAD*7 and *AtFAD*8 is also indicated. A diagram of the localization and distribution of putative *cis*-acting regulatory sequences found in both promoters using PLANTCARE and PLACE tools is also shown.

**Supplementary Figure 2.** (A) Determination of the *AtFAD7*, *AtFAD*8 and *AtFAD3* gene expression ratio in TG7 and TG8 plant lines with respect to Col0. Data represent means of at least three biological replicates. (B) Growth phenotype of TG7 and TG8 lines compared to Col0. Plants were grown for 4 weeks in a climatic chamber.

**Supplementary Figure 3.** Confocal microscopy analysis from leaves of transgenic lines carrying the empty vector pEN-R2F-L3. Analysis was performed either in 10 day cotyledonal leaves as well as from two week-old rosette leaves. Images show the overlay between the GFP and chlorophyll fluorescence channels. Bars correspond to 10 µm.

**Supplementary Figure 4.** Confocal microscopy analysis of the *At*FAD7 protein in roots from TG7 plants grown fully illuminated or with the root growth zone protected from light. Analysis was performed in roots from 7 d-old plants in which the root growth area of the MS plates was covered to avoid illumination (A and B) or kept under illumination (C and D). Merged images of GFP (green) and propidium iodide (red) fluorescence channels from root tip (A and C) and root (B and D). Bars correspond to 25 µm.

**Supplementary Figure 5.** Western blot analysis of the relative abundance of the *At*FAD8 protein in leaf and roots of TG8 lines. Protein extracts from leaves and roots from 14 day-old from TG8 transgenic lines grown in MS plates. To favor its detection in roots, 30-35 µg of total protein were loaded per lane. Anti-GFP was used as primary antibody. Coomasie staining of total proteins from both extracts is shown as loading control.

**Supplementary Figure 6.** RT-PCR of *LOX2* and *ABI1* genes as internal controls of the MeJA and ABA treatments applied in this work. ACTIN was used as housekeeping gene.

**Supplementary Figure 7.** (A) Confocal microscopy analysis of the relative abundance of the *At*FAD7 protein in TG7 transgenic lines in response to 100 µM ABA treatment. Bars correspond to 10 µm. (B) Confocal microscopy analysis of the relative abundance of both *At*FAD7 and *At*FAD8 proteins in TG7 and TG8 transgenic lines in response to cold treatment. Plants were maintained at 22 ºC or kept at 6 ºC for one week before the analysis. Bars correspond to 10 µm. Images show the overlay between the GFP and chlorophyll fluorescence channels.

**Supplementary Figure 8.** Co-localization analysis of FAD7-YFP and FAD8-YFP fusion proteins with FAD6-CFP by transient expression in *N. benthamiana* leaves. Upper panel FAD7-FAD6 co-localization; lower panel FAD8-FAD6 co´localization. (A and E) autofluorescence of the chlorophyll from plastids, (B and F) FAD6-CFP, (C and G) FAD7-YFP and FAD8-YFP signals, respectively; (D and H) merged image from A,B , C and F,G,H, respectively. Scale bar is 10 µm in all pictures.

**Table 1**. Fatty acid composition of total lipids from roots of Col-0 and different fatty acid desaturase mutant lines.

| | Col-0 | *fad3-1* | *fad7i* | *fad8i* | *fad7-2/fad8-1* |
|---|---|---|---|---|---|
| C14:0 | 0,58 ± 0.11 | 0,54 ± 0.1 | 0,95 ± 0.4 | 0,52 ± 0.1 | 0,52 ± 0.2 |
| C16:0 | 23,85 ± 0.21 | 23,84 ± 0.4 | 29,53 ± 0.45 | 23,72 ± 0.55 | 24,37 ± 0.42 |
| C16:1 | 0,98 ± 0.25 | 0,72 ± 0.17 | 0,76 ± 0.07 | 0,7 ± 0.14 | 0,52 ± 0.1 |
| C18:0 | 4,21± 0.18 | 4,67 ± 0.16 | 7,94 ± 0.23 | 3,42 ± 0.1 | 4,69 ± 0.31 |
| C18:1 | 4,76 ± 0.29 | 5,82 ± 0.32 | 4,68 ± 0.27 | 4,64 ± 0.14 | 4,39 ± 0.2 |
| C18:2 | 30,28 ± 0.54 | 53,35 ± 0.46 | 28,08 ± 0.24 | 30,13 ± 0.4 | 31,18 ± 0.59 |
| C18:3 | 23,06 ± 0.56 | 4,16 ± 0.01 | 21,01 ± 0.36 | 28,78 ± 0.56 | 26,04 ± 0.79 |
| C20:0 | 0,96 ± 0.1 | 0,45 ± 0.05 | 0,67 ± 0.01 | 0,73 ± 0.14 | 0,79 ± 0.14 |
| C20:1 | 0,22 ± 0.14 | 0,07 ± 0.02 | 0 | 0,32 ± 0.14 | 0,36 ± 0.1 |
| C22:0 | 6,59 ± 0.18 | 2,84 ± 0.17 | 2,99 ± 0.14 | 3,32 ± 0.24 | 3,56 ± 0.31 |
| C22:1 | 0,43 ± 0.17 | 0,41 ± 0.06 | 0,31 ± 0.14 | 0,46 ± 0.17 | 0,28 ± 0.17 |
| C24:0 | 3,74 ± 0.15 | 2,78 ± 0.24 | 3 ± 0.26 | 3,16 ± 0.1 | 3,22 ± 0.6 |

Data represent means from two biological replicates.

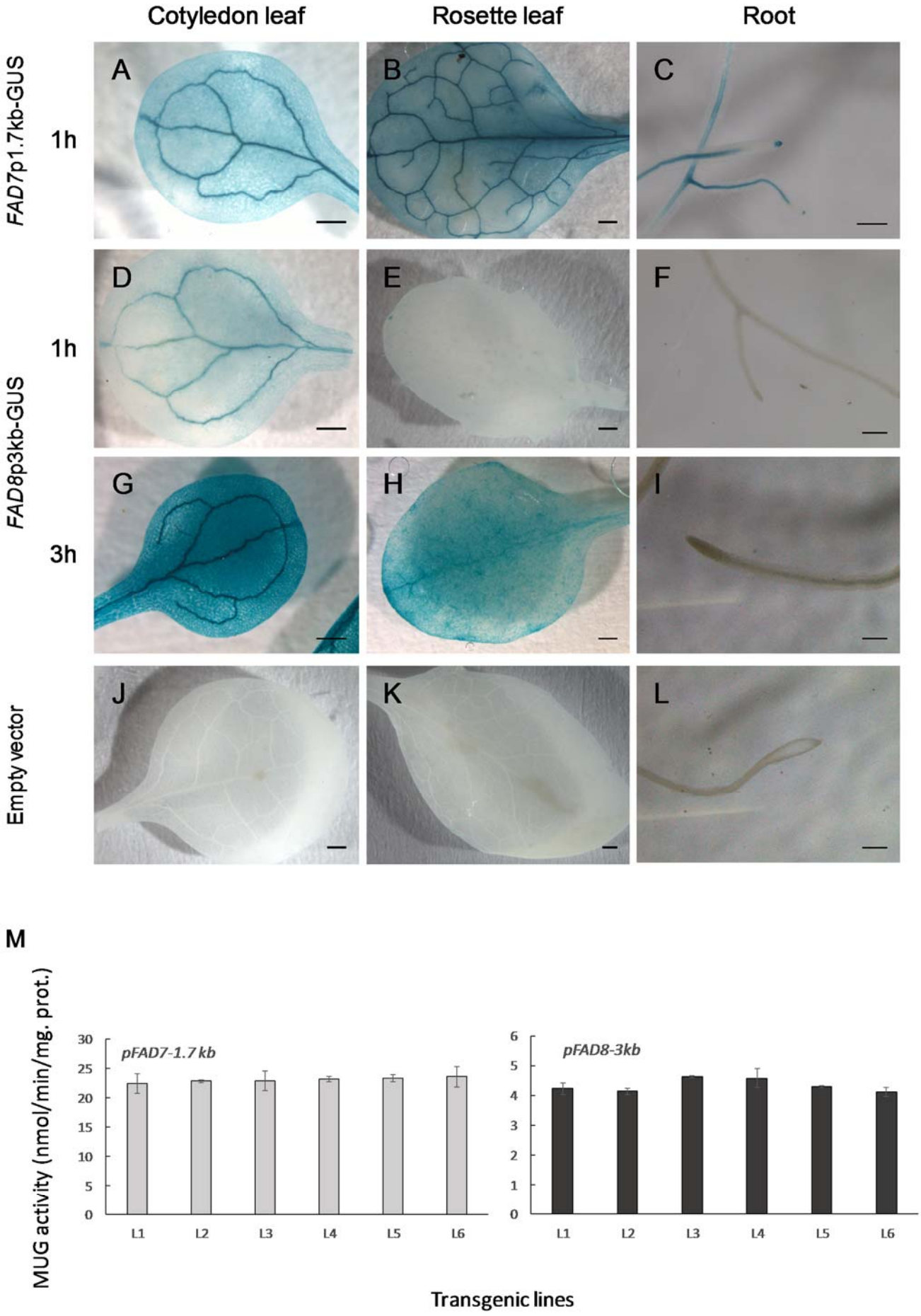


Soria et al., Figure 1

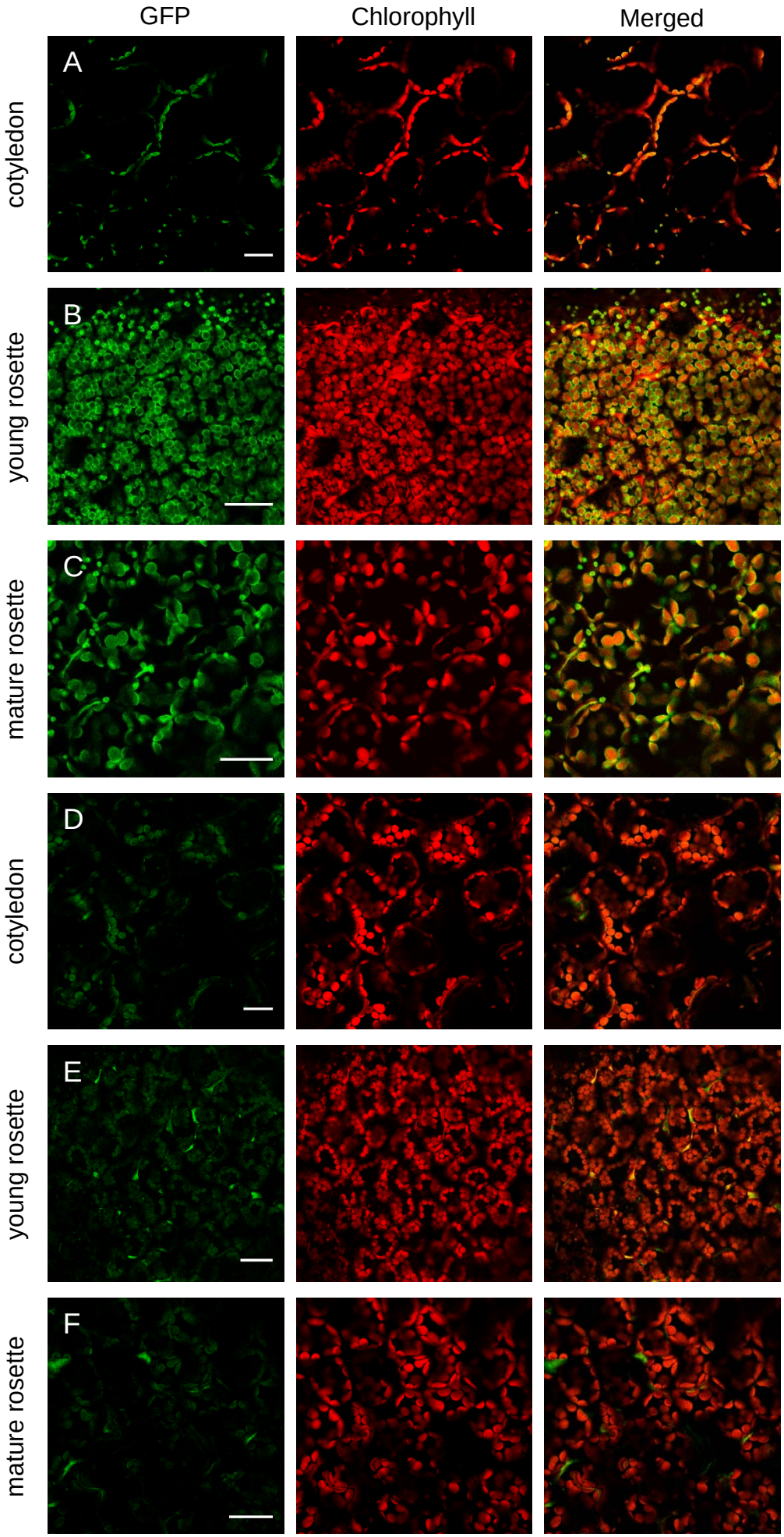


Soria et al., Figure 2

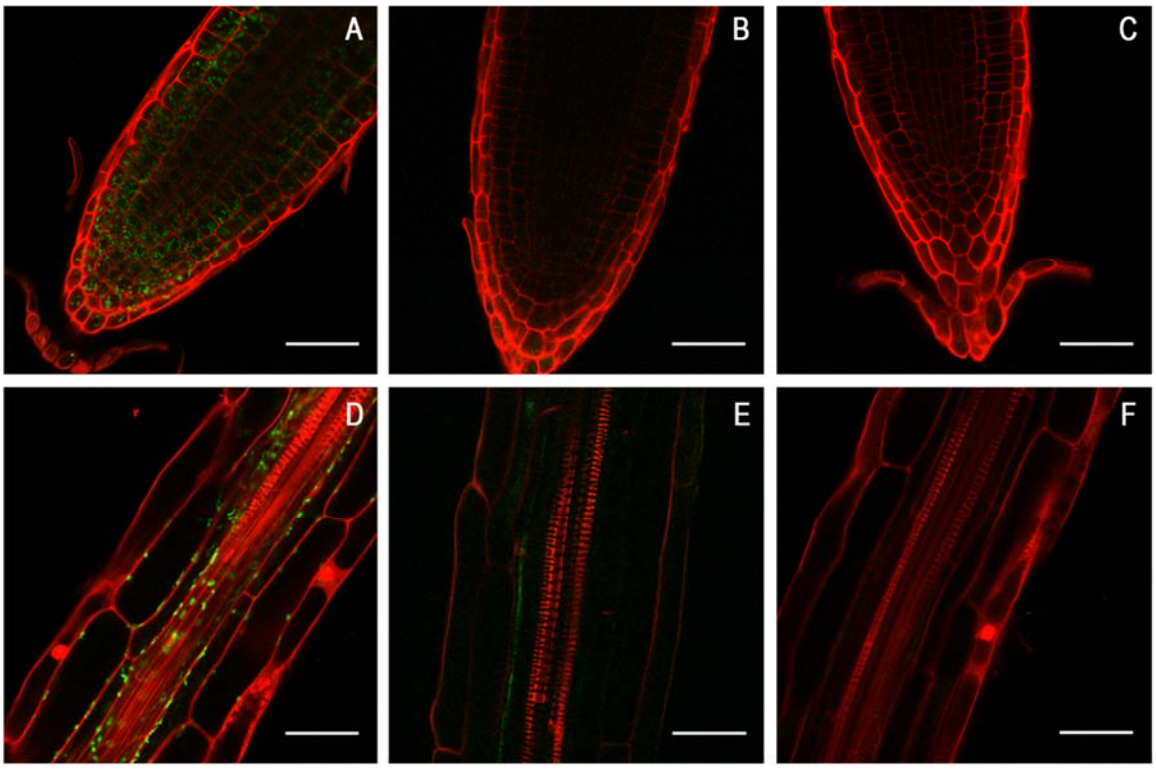


Soria et al., Figure 3

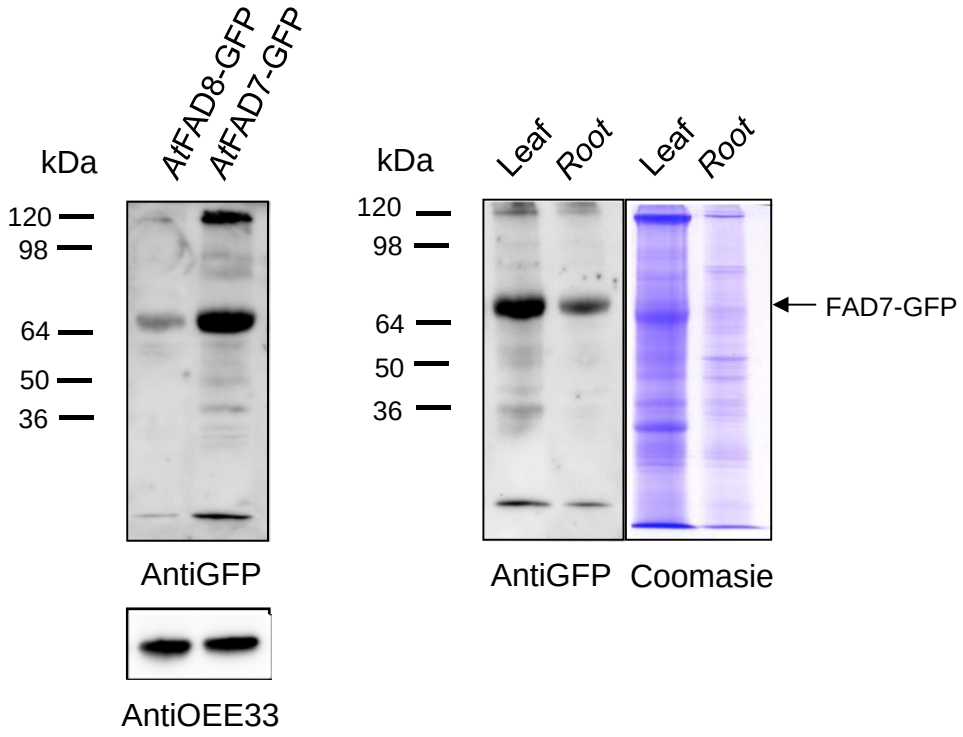


Soria et al., Figure 4

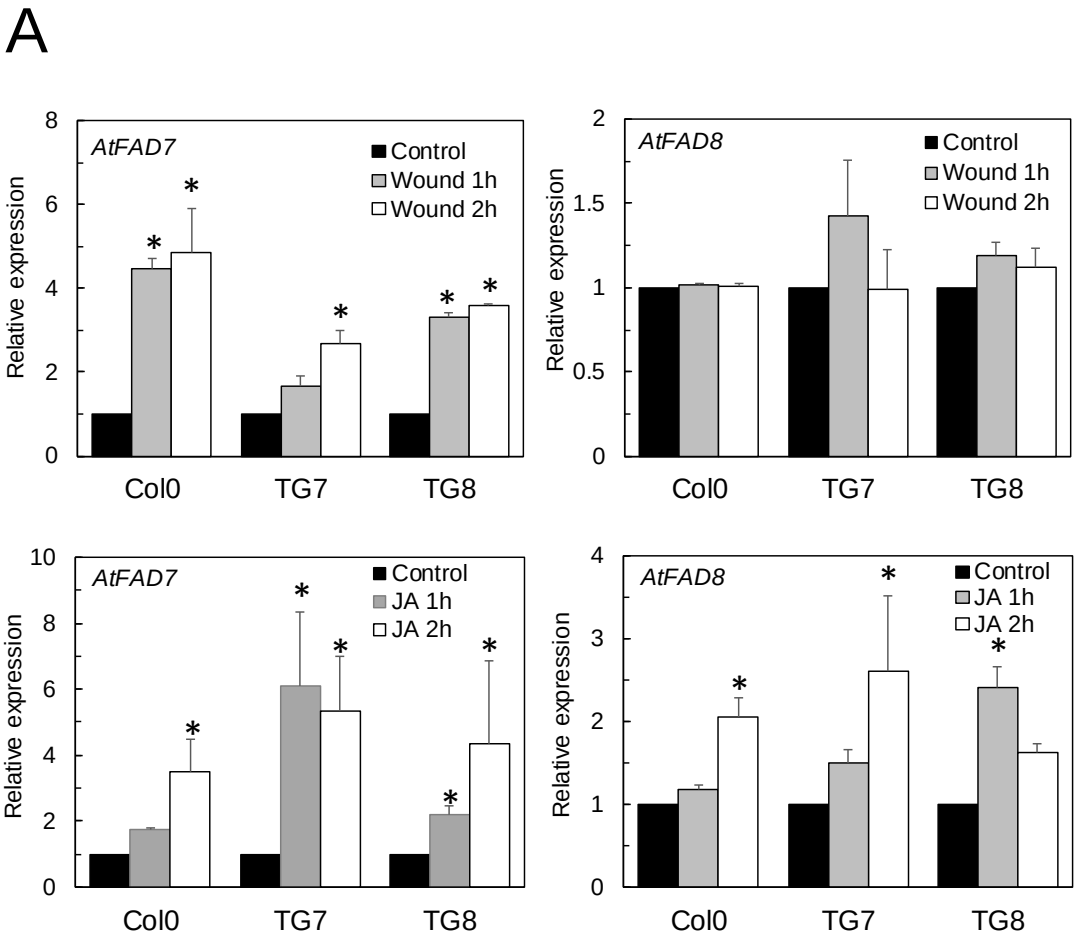


Soria et al., Figure 5

A

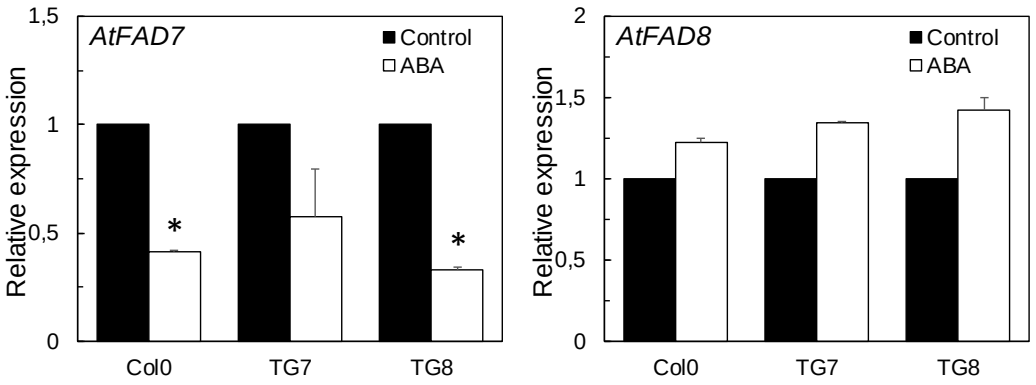


B

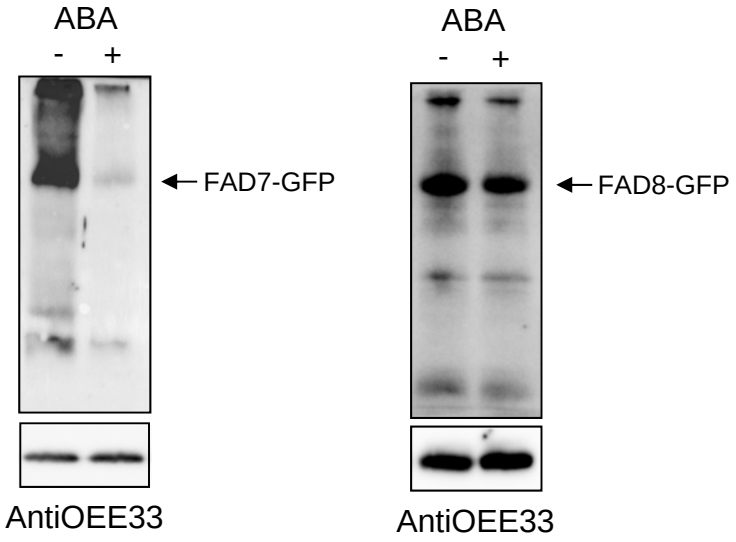


Soria et al., Figure 6

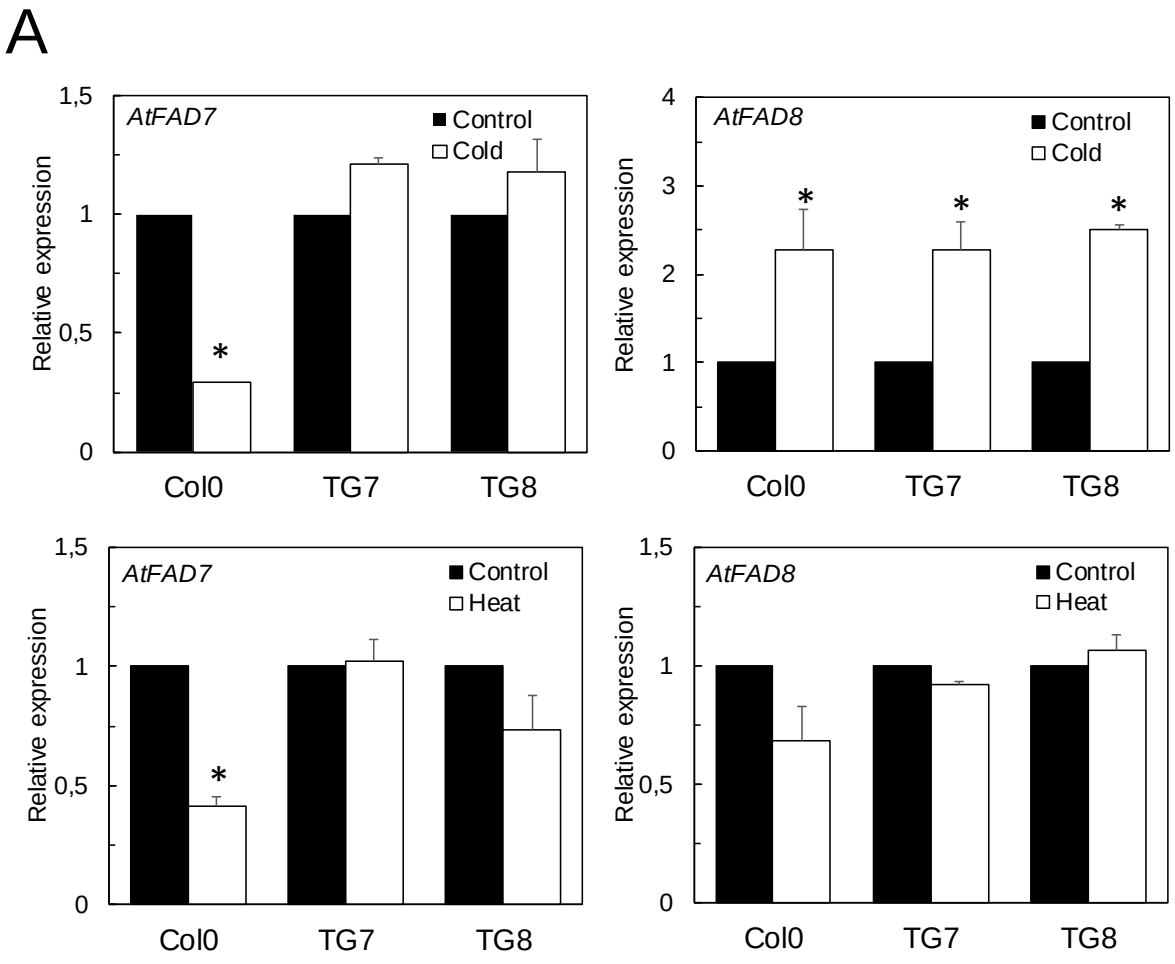


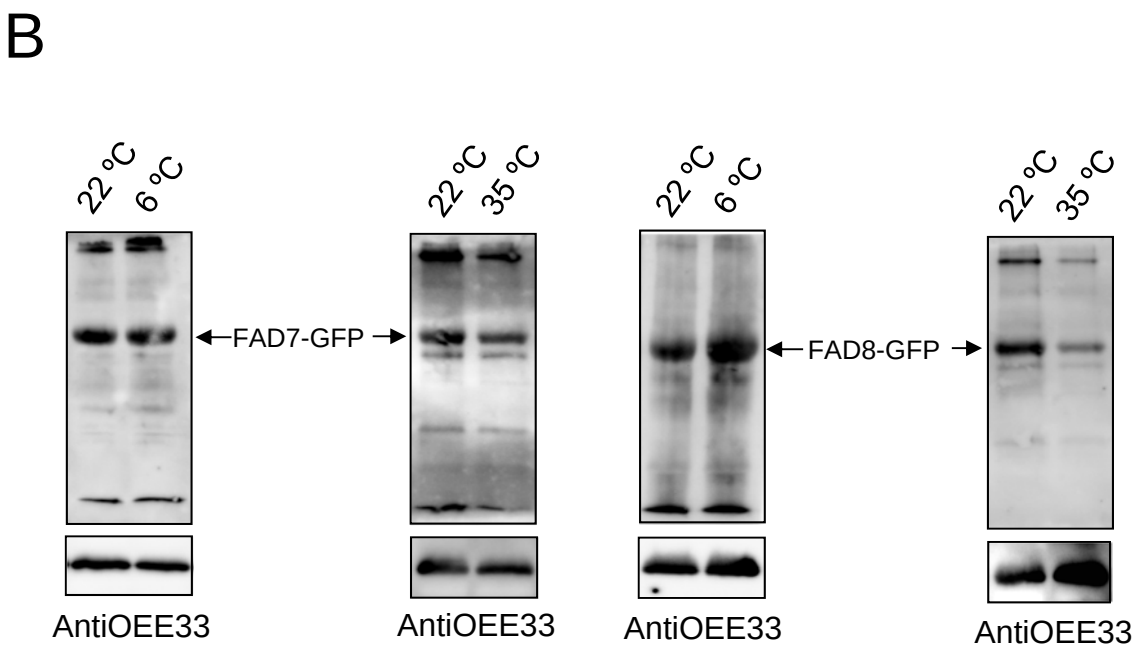


Soria et al., Figure 7

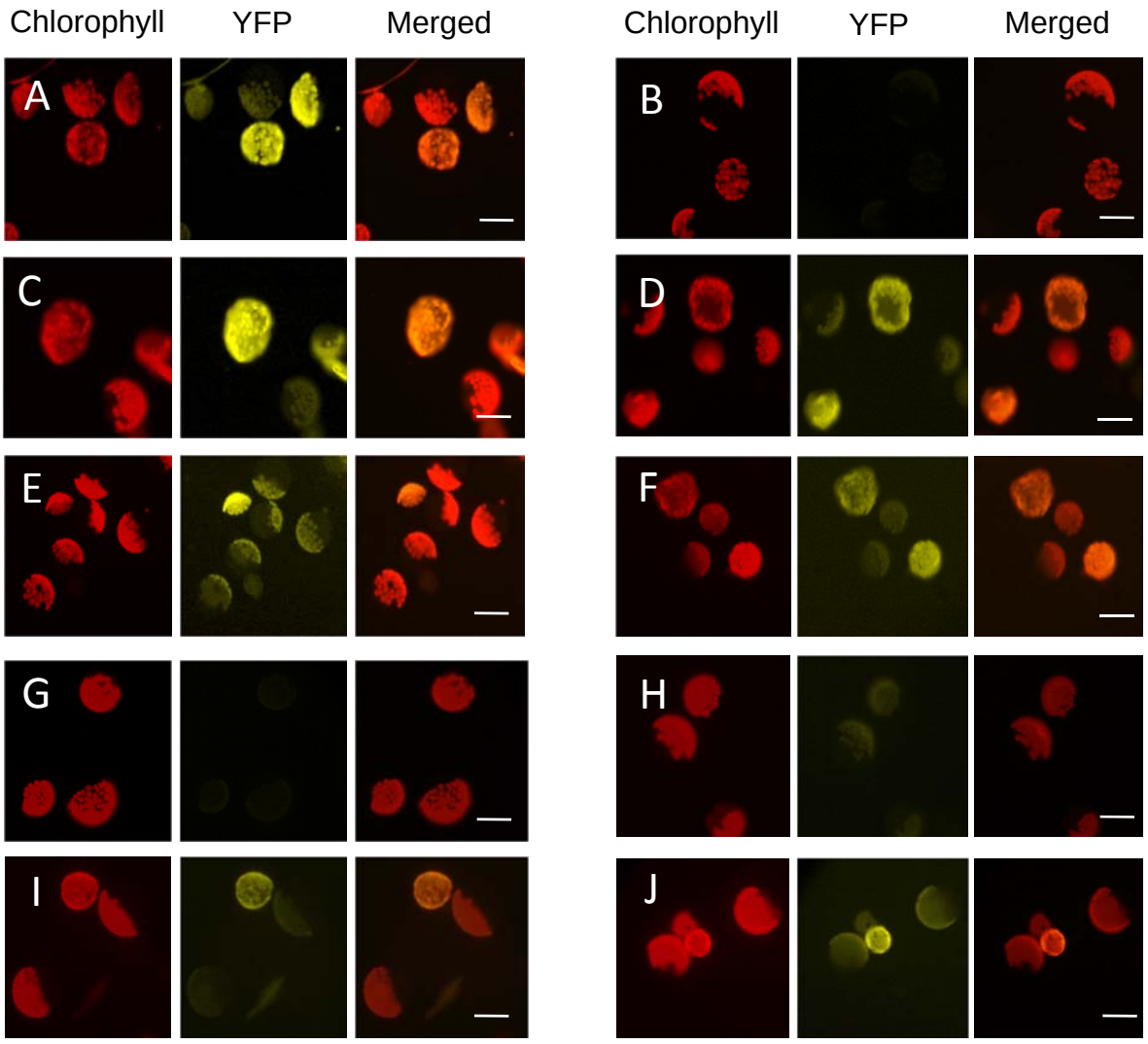


Soria et al., Figure 8

Dear Dr. Li-Beisson, Editor Plant Cell Physiology

We would like to thank the evaluation of our manuscript (PCP-2018-E-00272) that we sent for publication to Plant Cell Physiology. We would also like to thank the work by both reviewers for their valuable comments and suggestions. We have read their comments into detail. We have also performed most, if not all, the additional experiments suggested by the reviewers and taken into account their comments in the preparation of the revised version of the manuscript. Here are our detailed answers to their review.

*Reviewer 1.*

1.- The reviewer suggested the possibility of performing a lipid class analysis in root lipids to complement the results shown in Table 1 (fatty acid composition of total root lipids from the collection of mutants deficient in fatty acid desaturation). This might help to examine the role of *At*FAD7 in root lipid metabolism and therefore, help in the interpretation of our results.

With respect to the lipid class analysis suggested by the reviewer, we would like to mention that MGDG and DGDG are very minor components of root lipids; together they represent a 5% of total root lipids (*aralip.plantbiology.msu.edu*). In addition, we must bear in mind that a significant portion of both MGDG or DGDG present in root lipids may come from PC synthetized in the endoplasmic reticulum, desatured by FAD3 and later transported to the plastid in form of DAG. This DAG could be converted to 18:3 MGDG or DGDG in the plastid. Therefore, the results of the lipid class analysis might not be conclusive. This might also explain how 18:3 is synthetized in the absence of reduced ferredoxin, as stated by the reviewer. Cytochrome $b_5$ is the electron donor of FAD3. Nevertheless, our data clearly show that the *At*FAD7 protein is present in the root. Furthermore, both our GUS-staining data as well as the confocal microscopy localization analysis show a specific distribution in the root cap and adjacent to the root vasculature (Figs. 1 and 3). This suggests a relationship between its distribution and its function. In that sense, some genes that are involved in JA biosynthesis or signalling have a similar GUS-staining or distribution pattern in the root. Is the case of LOX9 (Hayashi et al., 2008) or JAZ1 (Meesters et al., 2014), to cite two examples. These results open the possibility that the role of *At*FAD7 in roots might be more related with JA biosynthesis than the mere TA biosynthesis for membrane lipids. However, we cannot discard this activity. Galactolipids are very minor lipids in the root. Although we did not detect 16:3 in our analysis, others (Beaudoin et al., 2009) detected a 1,5 % of 16:3 in total lipids from roots. This very minor 16:3 could only be originated from the activity of *At*FAD7.

We feel that this question was not well explained in the previous version of the paper. Accordingly, some of the arguments mentioned above have been included in the discussion section (P19, L20-25 and P20, L1-10) of the revised version of the paper for a better comprehension of our data and conclusions.

2.- The reviewer asked for a second technique that might support the BiFC analysis. Yeast double-hybrid analysis could be used to monitor these interactions. However, the fact that *At*FAD7, *At*FAD8 and *At*FAD6 are plastid membrane integral proteins that are

inserted in a galactolipid enriched membrane, absent in yeast, might cause incorrect insertion/folding problems that may complicate the analysis. In parallel to the BiFC experiments shown in the previous version of the manuscript, we performed a co-localization analysis of both *At*FAD7, *At*FAD8 and the ω-6 desaturase *At*FAD6 to analyze the distribution of these complexes in the plastid membrane. This analysis was based in the co-transformation of *N. benthamiana* leaves with both *At*FAD7-YFP or *At*FAD8-YFP proteins with a *At*FAD6-CFP construct and detection by confocal microscopy of both proteins. The results suggested that both *At*FAD7/*At*FAD8 and *At*FAD6 were located in close vicinity in the membrane and might be consistent with the BiFC data. These new results are included in the revised version of the manuscript as a supplementary figure 8 and on P18, L3-21 of the revised version of the manuscript.

Other comments from this reviewer:

1.- The reviewer asked for an explanation of why we choose the promoter fragments used for our analysis. It is frequent that many promoter analysis use a 2 kb fragment upstream the ATG assuming that all the regulatory elements involved in gene expression are within this fragment. In our case, before initiating our research, we performed an exhaustive search of putative regulatory elements in the upstream sequences from both promoters. This search provided us with information of the location of specific *cis*-acting sequences in both promoters, some of them (more concretely two putative MYB sites, present in both gene promoters) located at long distance from the ATG (particularly in the case of *AtFAD8*). *A priori*, we could not discard any of these putative regulatory sequences and this is why we choose both promoter fragments with different length. In this regard, we would like to mention that there is work in progress from our group in which specific deletions in both promoter sequences have been performed and their involvement in basal expression as well as in response to stress or hormones has been analyzed. Our data show that some of the regions containing these putative regulatory sequences (including the distal ones) might be involved in these responses. This is why we feel that the election of the sequences was accurate. To better illustrate this, we have introduced in the revised version of the manuscript a modified Supplementary Figure 1 that, in addition to the specific chromosome localization of both promoter sequences, includes a schematic diagram showing the precise location of these putative regulatory elements. In parallel, more emphasis in the fact that the length of the promoter fragments was made after the bioinformatic analysis has been added in the text of the revised version of the manuscript, P8, L1-6. We hope that this additional explanation may help to clarify our decision.

2.- Following the advice of the reviewer, GUS promoter activity in addition to GUS staining data have been included in the revised version of the manuscript.

3.- We agree with the reviewer that the former expression data were misleading. We have eliminated this figure in the revised version of the manuscript (that has been substituted by the GUS activity data) and in the rest of the qPCR experiments shown in the paper, comparisons among different genes have been avoided.

4.- The reviewer asked for the strong GFP signal associated with small chloroplasts. We agree with the reviewer that they do not have the chloroplast shape of the rest of the chloroplast shown in the photographs, but they contain chlorophyll (red fluorescence).

The separation of the channels, as suggested by the reviewer, has been very useful to assess this. In addition, to favor the interpretation of our data, we are showing in this revised version of the manuscript bigger area photographs that we feel provide a more accurate information. It is also true, as stated by the reviewer that they seem to be specific of *At*FAD7-GFP lines since no signal was detected in the *At*FAD8-GFP plants. This is mentioned in P. 10, L16-20 of the revised version of our work.

5.- Following the advice of the reviewer we have included a high-temperature (35 ºC) experiment in the revised version of the manuscript, complementing the cold data of the previous version. Our data show that high temperatures seemed not to affect *At*FAD7 both at the transcript and protein levels. This result was consistent with previous observations from Matsuda and coworkers, cited by the reviewer. On the contrary, *At*FAD8 protein levels clearly decreased at 35 ºC (without changes in transcript levels) in opposition to what happened at cold temperatures. This was also consistent with previous data from Matsuda et al., (2005). Our data indicate that both proteins have different sensitivity to temperatures. In the paper we hypothesized that these differences could be related with the higher specialization of *At*FAD8 in PG desaturation and the role of this lipid class in temperature tolerance and acclimation (P21, L19-21). The high temperature experiments are included in P16, L19-24 and P17, L1-4 of the revised version of the text.

6 and 7.- All the rest of the minor comments of the reviewer have been corrected in the revised version of the text.

*Reviewer 2.*

The reviewer asked whether we have determined changes in *AtFAD7* or *AtFAD8* expression ratio in our transgenic lines with respect to the wild-type plants in order to evaluate possible secondary effects of the expression of the transgene in our transgenic lines. He also wondered whether the expression of the transgene produced any alterations in the phenotype of our transgenic plants. We have introduced these results in the revised version of the manuscript. Most of the transgenic lines expressing the *At*FAD7 protein fused to GFP under the control of the 1,7 kb promoter analysed showed an increase in *AtFAD7* expression of 2-3 fold on average when compared to Col0 plants. Similarly, transgenic lines expressing the *At*FAD8-GFP protein under the expression of the 2,9 kb promoter showed a 2-fold average increase in *AtFAD8* mRNA when compared to Col0 lines. Interestingly, the expression of both transgenes did not affect the expression of the other plastidial desaturase counterpart or those from the endoplasmic reticulum ω-3 desaturase FAD3. Introduction of the transgene did not induce any modifications of the phenotype of the transgenic lines in terms of growth, development, flowering or seed germination. All these results have been included in the revised version of the manuscript as a supplementary figure 2, and described in the text, Results section, P9, L15-25 and P10, L1-6.

Other comments:

1.- Fig.1M (O in the previous version of the paper); the reviewer asked not to compare the expression levels of *AtFAD7* and *AtFAD8* genes as shown in this figure, since it was

not correct. This was also mentioned in the comments of reviewer 1. We agree with the comment of the reviewer. The figure has been eliminated and substituted by the determination of GUS activity in the revised version of the manuscript, as requested by both reviewers. Similarly, comparison among genes in the different treatments of our work has been avoided.

2.- The question of the small chloroplasts containing a strong GFP signal has been also answered in the comments to reviewer 1. As mentioned by reviewer 2, these small chloroplasts containing GFP were more abundant in young rosette leaves (Fig. 2B) than in mature ones (Fig. 2C), suggesting that their presence was somewhat related with leaf age/maturation. The reviewer asked why they were not seen in former Fig 2E (young rosette leaves from *At*FAD8-GFP lines). The co-localization of the GFP signal with these small chloroplasts was specific of the *At*FAD7-GFP lines (Figs. 2B and 2C of the revised manuscript). However, the small chloroplast structures with red chlorophyll fluorescence were also detected in the *At*FAD8-GFP lines (Fig. 2E). Here, very low if any GFP signal was detected, consistent with the very low GFP signal of the *At*FAD8-GFP lines.

3.- Significance of the data is shown with an asterisk in the qPCR expression data as requested by the reviewer.

4.- Following the advice of the reviewer we have introduced the qPCR expression data from TG7 and TG8 lines in addition to those from Col0 plants in all the experimental treatments analysed in our work. We must apologize for not including them in the previous version of the manuscript. They were required for a good interpretation of the protein data as stated by reviewer 2. New figures, 5, 6 and 7 are provided including the data requested by the reviewer.

5.- As requested by the reviewer, a loading control has been included in the western blot data. We have decided to use as a loading control an antiOEE33 antibody, which recognizes the 33 kDa extrinsic oxygen evolving complex protein from Photosystem II, which is a good marker of plastidial proteins as are *At*FAD7 and *At*FAD8. In the case of the comparison between leaf and root tissues, we decided to include a coomasie brilliant blue (CBB) staining of total proteins from the replica-gel used for western blotting. This was also available for all the blots shown in the paper, but we decided to use the antiOEE33 as marker for a better structure of the figures when leaf samples were analysed. These results are shown in the new Figs. 5, 6 and 7 of the revised version of the manuscript and description has been modified in the methods section P30, L8-11. In addition, we have deleted the confocal photographs of the treatments and inserted them in a new supplementary Figure 7. We decided to do this since the changes in relative abundance were already shown in the western blot and no changes in protein distribution were detected with the confocal microscopy analysis. However, they are still available for readers as supplementary Figure 7.

6.- As requested by the reviewer the effect of ABA on *At*FAD8 was also performed. Both *AtFAD8* expression and protein levels have been analysed and compared with those of *At*FAD7. Our data suggest that conversely to what happened with *AtFAD7*, the *AtFAD8* gene was not sensitive to ABA. This might be consistent with the presence of two putative ABA repression sequences in the *AtFAD7* gene promoter that are not present in the *AtFAD8* one. These new results are included in the new figure 6 of the

revised version of the manuscript and described in the results section P14, L22-25 and P15 L1-16.

7.- The reviewer asked to discuss more deeply the significance of wound-sensitive/JA-insensitive genes as shown for the case of our *AtFAD7* and *AtFAD8* genes, respectively. The existence of wound-sensitive/JA-insensitive genes has been reported extensively in the literature. These results were obtained in the differential display analysis of wound and JA inducible genes (Titarenko et al., 1997) or more recently in the microarray analysis of wound-, JA, and OPDA-regulated genes (Taki et al., 2005), to cite two examples. To our knowledge, the reasons for the existence of this different behaviour are not clear. In an excellent review, Howe (2004) details a possible explanation for this behaviour. Thus, two subsets of genes would be activated in defence responses. A first subset of genes would be activated locally in a mechanism independent of JA perception and signalling. These genes might provide a rapid defence response. The second group of genes might be activated more systemically in the rest of the rosette and should require both JA biosynthesis and perception. The existence of this dual wound perception profile will ensure a rapid response even when JAs are still low and a sustained response time after the wound/infection. Whether *AtFAD7* and *AtFAD8* fall within this schema is difficult to assess. *AtFAD8* might be assigned to this second group of genes that are activated systemically rather than locally by JA. On the contrary, *AtFAD7* could be ascribed to the first subset of genes. Nevertheless, a precise assignment might require other experiments that might include infection, herbivore attack experiments or supplementation with jasmonates other than JA like OPDA or even dnOPDA, not object of theis work. Nevertheless, following the reviewer advice, we have introduced this question in the discussion section, P20, L20-25 and P21, L1-2 of the revised version of the manuscript.

8.- Following the reviewer advice we have shortened the discussion section of the paper.

9.- Other minor points stated by the reviewer concerning the spelling of some words have been corrected in the revised version of the manuscript.

We hope that this revised version of the manuscript could be acceptable for publication in *Plant Cell Physiology*.

Kind regards,

Miguel Alfonso.
EEAD-CSIC